

AD-753 101

IMPACT STRENGTH AND TOUGHNESS OF FIBER
COMPOSITE MATERIALS

Lawrence J. Broutman, et al

Illinois Institute of Technology

Prepared for:

Air Force Office of Scientific Research

November 1972

DISTRIBUTED BY:

NTIS

National Technical Information Service
U. S. DEPARTMENT OF COMMERCE
5285 Port Royal Road, Springfield Va. 22151

AFOSR Scientific Report
AFOSR TR-72-2289

AD753101

Air Force Office of Scientific Research

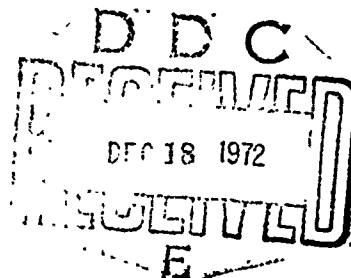
Grant AFOSR 72-2214

Technical Report No. 1

**IMPACT STRENGTH AND TOUGHNESS
OF FIBER COMPOSITE MATERIALS**

by

L. J. Broutman and A. Rotem



Department of Metallurgical and Materials Engineering
ILLINOIS INSTITUTE OF TECHNOLOGY
Chicago, Illinois 60616

November 1972

Reproduced by
NATIONAL TECHNICAL
INFORMATION SERVICE
U S Department of Commerce
Springfield VA 22151

Approved for public release; distribution unlimited

55

Qualified requestors may obtain additional copies from the Defense Documentation Center, all others should apply to the National Technical Information Service.

Reproduction, translation, publication, use and disposal in whole or in part by or for the United States Government is permitted.

1. NAME _____
 2. ADDRESS _____
 3. CITY _____
 4. STATE _____
 5. ZIP _____
 6. PHONE _____
 7. DATE _____
 8. TIME _____
 9. BY _____
 10. REMARKS _____
 11. INITIALS _____
 12. SIGNATURE _____
 13. DATE _____
 14. TIME _____
 15. BY _____
 16. REMARKS _____
 17. INITIALS _____
 18. SIGNATURE _____
 19. DATE _____
 20. TIME _____
 21. BY _____
 22. REMARKS _____
 23. INITIALS _____
 24. SIGNATURE _____
 25. DATE _____
 26. TIME _____
 27. BY _____
 28. REMARKS _____
 29. INITIALS _____
 30. SIGNATURE _____
 31. DATE _____
 32. TIME _____
 33. BY _____
 34. REMARKS _____
 35. INITIALS _____
 36. SIGNATURE _____
 37. DATE _____
 38. TIME _____
 39. BY _____
 40. REMARKS _____
 41. INITIALS _____
 42. SIGNATURE _____
 43. DATE _____
 44. TIME _____
 45. BY _____
 46. REMARKS _____
 47. INITIALS _____
 48. SIGNATURE _____
 49. DATE _____
 50. TIME _____
 51. BY _____
 52. REMARKS _____
 53. INITIALS _____
 54. SIGNATURE _____
 55. DATE _____
 56. TIME _____
 57. BY _____
 58. REMARKS _____
 59. INITIALS _____
 60. SIGNATURE _____
 61. DATE _____
 62. TIME _____
 63. BY _____
 64. REMARKS _____
 65. INITIALS _____
 66. SIGNATURE _____
 67. DATE _____
 68. TIME _____
 69. BY _____
 70. REMARKS _____
 71. INITIALS _____
 72. SIGNATURE _____
 73. DATE _____
 74. TIME _____
 75. BY _____
 76. REMARKS _____
 77. INITIALS _____
 78. SIGNATURE _____
 79. DATE _____
 80. TIME _____
 81. BY _____
 82. REMARKS _____
 83. INITIALS _____
 84. SIGNATURE _____
 85. DATE _____
 86. TIME _____
 87. BY _____
 88. REMARKS _____
 89. INITIALS _____
 90. SIGNATURE _____
 91. DATE _____
 92. TIME _____
 93. BY _____
 94. REMARKS _____
 95. INITIALS _____
 96. SIGNATURE _____
 97. DATE _____
 98. TIME _____
 99. BY _____
 100. REMARKS _____
 101. INITIALS _____
 102. SIGNATURE _____
 103. DATE _____
 104. TIME _____
 105. BY _____
 106. REMARKS _____
 107. INITIALS _____
 108. SIGNATURE _____
 109. DATE _____
 110. TIME _____
 111. BY _____
 112. REMARKS _____
 113. INITIALS _____
 114. SIGNATURE _____
 115. DATE _____
 116. TIME _____
 117. BY _____
 118. REMARKS _____
 119. INITIALS _____
 120. SIGNATURE _____
 121. DATE _____
 122. TIME _____
 123. BY _____
 124. REMARKS _____
 125. INITIALS _____
 126. SIGNATURE _____
 127. DATE _____
 128. TIME _____
 129. BY _____
 130. REMARKS _____
 131. INITIALS _____
 132. SIGNATURE _____
 133. DATE _____
 134. TIME _____
 135. BY _____
 136. REMARKS _____
 137. INITIALS _____
 138. SIGNATURE _____
 139. DATE _____
 140. TIME _____
 141. BY _____
 142. REMARKS _____
 143. INITIALS _____
 144. SIGNATURE _____
 145. DATE _____
 146. TIME _____
 147. BY _____
 148. REMARKS _____
 149. INITIALS _____
 150. SIGNATURE _____
 151. DATE _____
 152. TIME _____
 153. BY _____
 154. REMARKS _____
 155. INITIALS _____
 156. SIGNATURE _____
 157. DATE _____
 158. TIME _____
 159. BY _____
 160. REMARKS _____
 161. INITIALS _____
 162. SIGNATURE _____
 163. DATE _____
 164. TIME _____
 165. BY _____
 166. REMARKS _____
 167. INITIALS _____
 168. SIGNATURE _____
 169. DATE _____
 170. TIME _____
 171. BY _____
 172. REMARKS _____
 173. INITIALS _____
 174. SIGNATURE _____
 175. DATE _____
 176. TIME _____
 177. BY _____
 178. REMARKS _____
 179. INITIALS _____
 180. SIGNATURE _____
 181. DATE _____
 182. TIME _____
 183. BY _____
 184. REMARKS _____
 185. INITIALS _____
 186. SIGNATURE _____
 187. DATE _____
 188. TIME _____
 189. BY _____
 190. REMARKS _____
 191. INITIALS _____
 192. SIGNATURE _____
 193. DATE _____
 194. TIME _____
 195. BY _____
 196. REMARKS _____
 197. INITIALS _____
 198. SIGNATURE _____
 199. DATE _____
 200. TIME _____
 201. BY _____
 202. REMARKS _____
 203. INITIALS _____
 204. SIGNATURE _____
 205. DATE _____
 206. TIME _____
 207. BY _____
 208. REMARKS _____
 209. INITIALS _____
 210. SIGNATURE _____
 211. DATE _____
 212. TIME _____
 213. BY _____
 214. REMARKS _____
 215. INITIALS _____
 216. SIGNATURE _____
 217. DATE _____
 218. TIME _____
 219. BY _____
 220. REMARKS _____
 221. INITIALS _____
 222. SIGNATURE _____
 223. DATE _____
 224. <

UNCLASSIFIED

Security Classification

DOCUMENT CONTROL DATA - R & D

(Security classification of title, body of abstract and indexing annotation must be entered when the overall report is classified)

1. ORIGINATING ACTIVITY (Corporate author) ILLINOIS INSTITUTE OF TECHNOLOGY DEPARTMENT OF METALLURGICAL AND MATERIALS ENGINEERING CHICAGO, ILLINOIS 60616		2a. REPORT SECURITY CLASSIFICATION UNCLASSIFIED	
3. REPORT TITLE IMPACT STRENGTH AND TOUGHNESS OF FIBER COMPOSITE MATERIALS		2b. GROUP	
4. DESCRIPTIVE NOTES (Type of report and inclusive dates) Scientific Interim			
5. AUTHOR(S) (First name, middle initial, last name) LAWRENCE J BROUTMAN ASSA ROTEM			
6. REPORT DATE Nov 1972		7a. TOTAL NO. OF PAGES 49	7b. NO. OF REFS 11
8a. CONTRACT OR GRANT NO. AFOSR 72-2214		9a. ORIGINATOR'S REPORT NUMBER(S)	
b. PROJECT NO. 9782-02		9b. OTHER REPORT NO(S) (Any other numbers that may be assigned this report) AFOSR-TR-72-2289	
c. 61102F			
d. 681307			
10. DISTRIBUTION STATEMENT Approved for public release; distribution unlimited.			
11. SUPPLEMENTARY NOTES TECH, OTHER		12. SPONSORING MILITARY ACTIVITY AF Office of Scientific Research (NAM) 1400 Wilson Boulevard Arlington, Virginia 22209	
13. ABSTRACT In recent years the development of advanced high performance fiber composite materials was mainly concerned with achieving high modulus and strength materials. However, high strength and stiffness by themselves may not be adequate for many structural applications as this combination of properties usually produces a brittle material. For example, carbon fiber composites possess superior stiffness and strength to weight ratios, but are quite brittle and have very low energy absorption capability. During this first year the energy absorption capability of glass fiber and carbon fiber composites has been studied by performing instrumented drop weight impact tests on beams. A drop weight impact machine was designed and built for this purpose. The strength and energy absorption of the composite beams has been measured as a function of impact velocity, impact mass, beam geometry, and also as a function of several composite material parameters. It has been shown that the strength and energy absorption of a beam are a function of impact velocity and the amount of energy supplied compared to the energy absorbed. The energy absorption is also a function of lamination plane orientation. Details of illustrations in this document may be better studied on microfiche			

DD FORM 1 NOV 66 1473

I

UNCLASSIFIED

Security Classification

Security Classification

14.

KEY WORDS

LINK A

LINK 8

LINK C

NAME	ROLE
Mr. J. Edgar Hoover	Director
Mr. Clegg	Chief of Bureau
Mr. Glavin	Chief of Bureau
Mr. Ladd	Chief of Bureau
Mr. Nichols	Chief of Bureau
Mr. Rosen	Chief of Bureau
Mr. Tracy	Chief of Bureau
Mr. Carson	Chief of Bureau
Mr. Egan	Chief of Bureau
Mr. Gurnea	Chief of Bureau
Mr. Hendon	Chief of Bureau
Mr. Pennington	Chief of Bureau
Mr. Quinn	Chief of Bureau
Mr. Nease	Chief of Bureau
Mr. Gandy	Chief of Bureau

WT

[illegible]

WT

NAME	ROLE
Mr. J. Edgar Hoover	Director
Mr. Clegg	Chief of Bureau
Mr. Glavin	Chief of Bureau
Mr. Ladd	Chief of Bureau
Mr. Nichols	Chief of Bureau
Mr. Rosen	Chief of Bureau
Mr. Tracy	Chief of Bureau
Mr. Carson	Chief of Bureau
Mr. Egan	Chief of Bureau
Mr. Gurnea	Chief of Bureau
Mr. Hendon	Chief of Bureau
Mr. Pennington	Chief of Bureau
Mr. Quinn	Chief of Bureau
Mr. Nease	Chief of Bureau
Mr. Gandy	Chief of Bureau

WT

COMPOSITES

II

Security Classification

AFOSR Scientific Report
AFOSR TR-

Air Force Office of Scientific Research
Grant AFOSR 72-2214
Technical Report No. 1

IMPACT STRENGTH AND TOUGHNESS
OF FIBER COMPOSITE MATERIALS

by

L. J. Broutman and A. Rotem

Department of Metallurgical and Materials Engineering
ILLINOIS INSTITUTE OF TECHNOLOGY
Chicago, Illinois 60616

November 1972

Approved for public release; distribution unlimited

III

FOREWORD

This research under Grant AFOSR 72-2214 was sponsored by the Air Force Office of Scientific Research, United States Air Force. Technical Supervisor for this program is Dr. Jacob Pomerantz, Project Scientist, Aeromechanics Division, Directorate of Aeromechanics and Energetics, Air Force Office of Scientific Research.

IV

IMPACT STRENGTH AND TOUGHNESS OF FIBER COMPOSITE MATERIALS

by L. J. Broutman* and A. Rotem**

Department of Metallurgical and Materials Engineering
Illinois Institute of Technology, Chicago, Illinois

1. INTRODUCTION

In recent years, the development of advanced high performance composite materials was mainly concerned with achieving high modulus and strength materials. But high strength is not sufficient, as some of the materials developed are of a brittle nature (the overall elongation to fracture is small), and one of the more important performance criterion should be the ability to absorb energy and resist impact loadings.

The energy absorption, or toughness of homogeneous isotropic materials has been measured by various techniques such as edge notched tensile tests, cleavage tests, Charpy, Izod and drop weight impact tests. The results obtained for brittle materials could often be correlated with fracture mechanics theories such as the Griffith theory for the fracture of brittle materials. However, when theories developed for simple materials are applied to fiber composites the behavior can not be predicted. The fracturing process for composites is much different from homogeneous materials and the energy absorption can certainly not be calculated by application of the "rule of mixtures" to the two or more phases. Thus, fracture theories were introduced suggesting fracture modes which include interface fracture, matrix fracture and the work done by the fibers as a crack passes perpendicular to them.⁽¹⁻⁵⁾

* Professor of Materials Engineering

** Post-Doctoral Research Associate (Present Address: Department of Materials Engineering, Technion, Israel Institute of Technology, Haifa, Israel)

To achieve an understanding of the fracture behavior of these materials and to construct more realistic models for analysis, the testing procedures used for simpler materials should not be assumed adequate for composites. More sophisticated test methods have already been introduced by investigators studying metals, for example, by modifying the Charpy Test Machine with instrumentation which records the load history.⁽⁶⁾ A more advanced technique used in impact testing was introduced by changing the method of impact to a drop weight and instrumented hammer or anvils.^(6,7)

The study of fibrous composite materials subjected to impact loading has not been given enough attention even though it should be a major design factor. The few published results on impact behavior were obtained with a standard Charpy impact machine without any attempt to study the phenomena of impact.⁽⁸⁻¹⁰⁾ For a fiber reinforced plastic material, it is likely that the impact behavior will be time dependent, i.e., dependent on the velocity of the hammer when striking the specimen. It has been shown that for a glass fiber reinforced plastic matrix, the ultimate strength increases as a function of the rate of loading in the fiber direction.⁽¹¹⁾ Thus, in this impact study, the rate of loading during impact was used as one of the primary variables. Drop weight impact studies on beams were performed, similar to a Charpy test. For these studies, a special apparatus was built in order that the impact process could be studied as a function of several experimental parameters, which are usually held fixed on commercial Charpy impact machines.

II. THE APPARATUS

The apparatus which was constructed to perform impact tests in bending is shown schematically in Fig. 1 and in a photograph in Fig. 2. The apparatus consists of a tubular frame 12 feet high with stainless steel guides attached to it. A drop weight with two cross members is capable of moving with a minimum of friction in the vertical direction. Teflon tips at the ends of the cross members insure the weight will stay in

its course. Different types of indenter tips can be attached to the drop weight, and its weight can be varied by adding weights on the drop weight shaft. A remote control hoist, with electromagnet at the end of the cable, is used to raise the weight to the desired height. The specimen is placed on two supports which have been designed to also serve as strain gage load cells. The supports can be moved to vary the span. The machine has been designed so that a high speed camera can be used from the side to photograph the process of fracture. The velocity of the indenter is measured just before striking the specimen by passing through infrared beams of two photo diodes, located one inch apart. These two photo diodes also trigger a time interval meter, and the lower one also triggers a storage oscilloscope which records the load cell response. After breaking the specimen, the weight passes through the beams of another two photo diodes, which trigger another time interval meter. Thus, the velocity of the weight just before and after striking the specimen is measured. The energy absorbed by the fracture of the specimen can be calculated* and the ultimate strength can be calculated from the oscilloscope load recording. A high speed movie camera located at the side of the apparatus and triggered by the photo device was used to photograph the fracture process at a framing rate of 6000 frames per second.

III. GLASS FIBER COMPOSITES

1. Experimental Procedures and Results

One of the composite materials selected for study was a nonwoven glass fiber reinforced epoxy resin. These materials were obtained either as laminates, fabricated by the 3M Co. or as pre-preg unidirectional tape which was fabricated into laminates in our own laboratory. Four types of specimens were used:

*The fracture energy was calculated from $E_f = \frac{W}{2g} \left[\left(\frac{S_1}{t_1} \right)^2 - \left(\frac{S_2}{t_2} \right)^2 \right] + WS_3$ where S_1 , S_2 and S_3 are the distance between the two upper photo devices, the two lower photo devices and the distance between the upper and the lower, respectively, t_1 and t_2 are the time interval measured, W is the weight of the drop, and g - the gravitational acceleration.

- (1) Scotchply type 1002 (E - glass in epoxy matrix) 25 plies with 0° - 90° lay up (cross plied).
- (2) Scotchply type 1002, 25 plies unidirectional lay up (1-2-19-2-1) with 4 plies at 90° .
- (3) Scotchply type 1002, 25 plies all unidirectional lay up.
- (4) Scotchply XP251S (S-glass in epoxy matrix) 18 plies, all unidirectional lay up.

The specimens were cut from the plates with a diamond wheel in various widths from $1/4$ " to 1" and in various lengths from 2.5" to 10".

The drop weight and the supports have tips with $1/4$ inch diameter. The supports were moved to the desired span and tightened on the slides. Locators were placed on the supports to adjust for the width of the specimen. The drop weight was raised by means of a winch to the selected height and then released from the electromagnet. Every test was performed at least five times. Tests were conducted primarily with unnotched specimens although a few tests were made with notched specimens. Experiments were also performed on a Charpy impact machine (11 ft./sec., 30 ft. lb.) to compare the results. For the quasi-static results, tests were performed on an Instron testing machine using the same type of specimens and loading conditions.

Fig. 3 shows the ultimate stress calculated from the load recording, versus the velocity of the drop weight just before striking the specimen (E-glass cross ply and unidirectional). Results are shown for the two drop weights, 6.34 lbs. and 12.68 lbs. The span was kept constant at 4 inches and the widths of specimens were $1/4$ ", $1/2$ " and 1". It can be seen that the fracture stress is not dependent on the weight as long as the energy is great enough to break the specimen, and also, not dependent on the specimen width. However, there is a 40% increase in the strength relative to the strength determined at a low rate of loading in the Instron testing machine.

Fig. 4 shows the energy absorbed by the specimens (E-glass/cross ply) versus the impact velocity, for various combinations of span, width and drop weight. The energy absorption is rate sensitive, the sensitivity dependent upon the above parameters. These results will be discussed later. Note that when the specimen width, span and the drop weight are doubled the curves have in some cases the same slope but never double the energy absorbed. Also note that just by changing the specimen width the level of the energy absorbed per unit width was hardly changed. Also shown in Fig. 4 is the region where the impact energy was not enough for complete fracture, and the region where no visual external damage was observed. For the zero rate, the energy was calculated as the area under the stress strain curve from an Instron test. It includes the total area under the curve till the load returns to zero.

Fig. 3 also shows the ultimate stress of the all-unidirectional specimens (3)* made from the pre-preg in our laboratory. The results are similar to those for the cross ply laminates, an increase of about 40% in the fracture stress compared to the quasi-static fracture stress. Again there is no effect by changing the drop weight or the width of the specimens (except in certain intervals as will be shown later). In Fig. 5 the results for energy absorption of the unidirectional specimens is plotted vs. the rate of loading. Different specimen widths are compared, and also the results for a Charpy test for the same specimen dimensions is shown. It can be seen that there is an increase in the amount of the energy absorbed with increasing impact velocity. The Charpy test seems to give lower results as do the widest one inch specimens (this phenomena is discussed later). Another phenomenon which occurred was transverse buckling of the specimen sides and this produces a high value of energy absorption as shown by the point in Fig. 5. This will also be discussed later. Fig. 6 shows the












* Number in parentheses refers to specimen number as shown on page 4.

ultimate stress for the 3M Co. fabricated unidirectional specimens (2) which shows the same behavior as the other materials having an increase in strength over the quasi-static value of about 40 percent. The results for S-glass specimens are shown in Figs. 6 and 7. The fracture stress is again higher than the quasi-static value but at longer spans (which gives actually a lower rate and a larger bending deflection) the fracture stress is not influenced by impact velocity. The energy absorbed is also rate sensitive as shown in Fig. 7.

The effect of the direction of loading relative to the lamination planes was also examined. Specimens were placed in the impact apparatus so that the lamination planes (the panel surface of the plate before cutting the specimens) were in the vertical direction. The results are shown in Fig. 8. While for the unidirectional, square cross-section specimens there is no difference in the results for either direction of loading, for the cross ply specimens there is a large difference. Furthermore, the cross ply specimens with the lamination planes vertical are not sensitive to the rate of loading. The Charpy test results for these specimens are also shown in Fig. 8 and agree with the general trend of the data. The lower energy absorption for the cross ply specimen with the lamination planes placed in a vertical position is a result of a different failure mode. This phenomena will be discussed later. Even though the energy absorption was lower, the fracture stress was the same for both specimen orientations.

The effect of a notch and specimen thickness was investigated and the results are presented in Table 1. The specimens were notch insensitive; when the energy absorbed was divided by the net cross-section area, the same results were obtained for notched and unnotched specimens. However, there is a large difference in the energy absorbed for the direction of loading with respect to the lamination planes and it is not linearly dependent on the cross-section area. To complete the information on the dimensional dependence, tests were made with different beam spans.

TABLE 1. The Effect of a Notch and Specimen Thickness on Energy Absorption

Material	Cross Section $\frac{in.}{b} \times \frac{in.}{h}$	Direction of Loading ↓	Span in.	Rate of Loading ft/sec.	σ_B ksj	E_f/b ft lb/in	E_f/A^* ft lb/in ²	Remarks
Cross Ply	1/4 x 1/2		3"	22.3	147	45.3	213.9	with notch**
Cross Ply	1/4 x 1/2		3"	16.0	170	45.1	220.5	with notch
Cross Ply	1/4 x 1/2		3"	16.0	147	56.3	224.3	unnotched
Cross Ply	1/2 x 1/4		3"	16.0	112	48.2	103.9	with notch
Cross Ply	1/2 x 1/4		3"	22.3	108	43.2	92.2	with notch
Cross Ply	1/2 x 1/4		3"	22.3	109	50.2	101.2	unnotched
Unidirectional	1/4 x 1/2		4"	22.3	177	78.9	290.5	unnotched
Unidirectional	1/2 x 1/4		4"	22.3	133	268.3	534.0	unnotched
S-glass, unidirectional	1/8 x 1/4		2"	22.3	261	36.5	293.9	unnotched
S-glass, unidirectional	1/8 x 1/4		3"	22.3	272	29.2	230.6	unnotched
S-glass, unidirectional	1/8 x 1/4		3"	22.3	173	718	293.5	unnotched

* h = specimen thickness, b = specimen width

A = cross-section area

** Notch Dimensions: Depth = 0.1 in.

Radius = 0.01 in.

Included angle = 45°

68

The results are shown in Fig. 9. Also appearing in Fig. 9 is the computed elastic energy which was stored in the specimen just before fracture.* It is seen that the absorbed energy is much greater than the stored elastic energy.

Tests were also performed on a high speed closed loop tension machine with controlled velocity. A bending fixture was adapted to the machine and specimens (unidirectional) of S-glass/epoxy were tested with 4" and 2" spans. Velocities of 10, 17 and 21.5 ft/sec. (1600 in/min) were used. Typical results from the oscilloscope are shown in Fig. 10. The straight line is the displacement record and the other line is the load. The results from the high speed tension machine were combined to form load deflection curves shown in Fig. 11. It is seen that the highest strength was achieved at the highest speed of loading, but the lower loading rate produced the higher energy absorption. When the photograph (Fig. 10) for the low rate of loading is carefully examined it is seen that at a deflection corresponding to 0.70 inches there is a disturbance on the curve, which can be correlated to the beginning of fracture. For the specimens tested at the higher rates ultimate fracture occurred at this deflection. The deflection is seen to be linear with time, but not the load. Because of the long span and the low modulus of the material, the specimen deflection is so great that the linear relation between load and deflection does not apply. For comparison, oscilloscope records taken from the impact apparatus show the same behavior. When the span was reduced to 2 inches, a linear relation between load and deflection

* The stored elastic energy was calculated from the maximum stress values, recorded on the oscilloscope when impacted, as follows:

$$E_f = \int_{P=0}^{P=\max.} P d\delta \quad . \text{ As } P \text{ was found to be almost a linear function of the deflection, then}$$

$$\text{elastic } E_f = \frac{1}{2} P \delta = \frac{(\sigma_{\max})^2 V}{216E} \quad \text{Ft. lb.}$$

where V = the volume of the specimen between the supports (in^3)
 E = the flexural modulus (psi)
 σ_{\max} = the maximum stress before failure (psi)

occurs as is seen in Fig. 12. Comparison between the results from the falling weight impact machine and the constant velocity test machine show that there is almost a constant rate of deflection achieved for the impact tests on the dropweight apparatus at these loading rates.

2. Discussion

The series of tests performed here show that adoption of test methods common for metals are not valid for nonmetallic composite materials. The standard Charpy test is not suitable for fiber glass epoxy composites as this material may not be sensitive to notches in either direction to the laminae, as seen from the results summarized in Table 1. More important, these materials are rate sensitive and so energy absorption values depend on the specific apparatus on which they are tested. From Figs. 3, 6, 7, and 11 we can see that the strength is increased as the rate of loading is increased, reaching a value of 40% over the quasi-static value for the rates considered. The energy absorbed during fracture also increases with increasing load rate, as seen from Figs. 4, 5, 7, and 9. But the fracture energy is very much dependent on the specific mechanism of fracture, which can vary from test to test even when all the parameters are kept constant. To illustrate this point, Fig. 13 shows some results for cross ply E-glass/epoxy laminates. The lower values, marked C.B. are associated with a type of fracture which looks like a sharp cut through the cross section with some spreading or "brooming" of the fibers near the cut. This type of fracture is thought to occur by crack propagation through the cross section while some delamination of the fibers occur as the crack passes perpendicular to them. A photograph of such failures is shown in Fig. 14. The higher energy absorption values marked with "T" are associated with a different kind of failure. As the specimen deflects, the outer layer is first fractured by tensile stresses but the crack does not propagate clearly perpendicular to the fibers; instead, extensive branching to the sides and delaminations along the fibers occurs. As the specimen continues to bend another layer is fractured in tension

and again the crack is stopped and delamination occurs. This process is continued until the remaining layer is thin enough to allow the specimen to bend excessively and slip between the supports. Such a failed specimen is also shown in Fig. 14 as well as a specimen which did not fail completely. For further examination of these failure mechanisms high speed photography was used. The series of pictures, taken at a speed of 6000 to 7000 frame/sec, shown in Fig. 15, illustrate this failure mechanism. Unfortunately, one cannot in advance tell which mechanism of failure will take place. When applying the load in a direction perpendicular to the laminae (lamination planes are vertical) of a cross-ply glass/epoxy laminate, a "cut" or "shear" type of failure is always obtained as can be seen in Fig. 16. The energy which is absorbed is very low as can be seen in Fig. 8. We can conclude that the energy needed to propagate a crack through the cross section, is much lower than the energy needed to form delaminations between the layers as the crack advances or pushes through the cross section. When unidirectional glass fiber/epoxy specimens were loaded with the lamination planes in a vertical position, the specimens buckled laterally (impact occurring at a low rate of loading) and high energy absorption resulted as shown in Fig. 5. This is also seen from Table 1, where the fracture energy for unidirectional specimens with the load applied in a direction perpendicular to the laminae, is double the energy absorbed for unit cross section with the lamination planes in a horizontal position. The failure mechanism in this case is buckling and delamination, as can be seen in Fig. 16. In Fig. 17 the buckling mechanism is shown by a series of pictures from the high speed movies. The compressive strength is lower than the tensile strength and thus buckling and delamination occur. It is clearly seen from Fig. 13 that the rate of loading does not determine which kind of fracture will occur, as both kinds occur for all the rates investigated. On the other hand when the load is applied in the perpendicular direction to a cross ply specimen, it always failed in a "cut" mode. This phenomena implies that the mode of fracture depends on the structure of the material through which the crack passes. In a

unidirectional or cross ply material! when the load is applied on the laminae face, internal voids, weak bonds between layers and local defects in the fibers can cause the crack to propagate through the cross section and create a "cut" failure, while if the opposite conditions exist the material can arrest the crack propagation, force the crack to branch to the sides and delaminate between the layers, thus absorbing much more energy and creating a "tension" failure as shown in Fig. 14.

Another important phenomena is the relation between the energy applied to the specimen and the energy which is absorbed when it fractures. It can be seen from Fig. 4, that for the same specimens, but different drop weights, the dependence on the rate of loading is greater for the smaller weight. In other words, the lower the ratio between the energy applied and the energy absorbed, the higher the dependence on the rate of loading. If we look at the same phenomena in Fig. 5 one can see that for the value of 50 ft.lb./in. the specimen did not fracture and for 55 ft.lb./in. it fractured with a high dependence on the rate of loading for this type of test. This phenomena occurs as a result of the change in the velocity of the drop weight while fracturing the specimen. When the energy applied is slightly larger than the energy which is needed to fracture the specimen, the attenuation of the velocity of the drop weight is large, and a large change in the rate of loading occurs during the test. But when the energy applied is much larger than the energy needed to fracture the specimen, there is only a slight change in the velocity and thus the results of the tests just show the dependence of the energy absorbed for a fixed rate of loading. To support this argument, the results from the impact apparatus are compared with the results from the high speed tension machine for which a constant velocity of the loading tip is achieved. We can see from Fig. 10 that actually we have the same constant rate of deflection from the impact apparatus as we have from the high speed tension machine, and from Fig. 12 that the load-time curve is almost linear. On the other hand when the energy applied is just somewhat larger than the

energy needed to break the specimen, the load-time curve which we get is as shown in Fig. 18. It can be seen that this is not a linear dependence, but the rate of loading decreases with time.

A very important result can be obtained by comparing the data in Figs. 4 and 5. The cross ply composite and the unidirectional composite absorb the same amount of energy. It is obvious from this result, that the mechanism of energy absorption is mainly by delamination, as the amount of fibers which fractured in a unidirectional specimen is double the amount fractured in a cross ply specimen. Moreover, comparing the data from Figs. 4 and 7 for the 1/8" thick specimens we see that the cross ply E-glass/epoxy and the unidirectional S-glass/epoxy also absorbed the same amount of energy. Hence it is obvious that the mechanism of absorbing energy is controlled by the amount of delamination between layers and between fibers and matrix. The fracture of the fibers themselves contribute only a small amount to the overall energy absorption.

3. Model of Fracture

Consider the loading of a beam supported at both ends, with a span long enough to create a tension failure mode on the tension side of the beam. The suggested failure modes for cases A, B and C are shown in Fig. 19.

Case A. The material is unidirectional, but consists of layers. The impact applied suddenly on the beam causes the beam to deflect (after the stress waves have decayed). As the loading continues a failure of the outer layer occurs at the mid point where the stress is maximum (or near it, at the weakest point). The crack tip propagates through the matrix material until it reaches the next layer of fibers and is arrested there. As the fibers in the first layer were broken a high shear stress exists in the matrix between these two layers which initiates cracks running to both sides parallel to the layers. Since the stress is decreasing toward the supports, the cracks will be

arrested after some distance. The impact is continued and when the stress in the second layer is high enough, the fibers will be broken and again a crack will propagate up to the third layer and branch to the side. Those cracks which run to the sides delaminating the specimen absorb the greatest amount of energy during the failure process.

Case B. The material is a cross ply laminate with the lamination planes in the horizontal direction. The same mechanism is valid here, except that there are less layers to arrest the propagating crack. Since in the unidirectional case, delamination did not occur at every layer, in the cross ply case approximately the same number of branching cracks occur as in the unidirectional composite. Hence the amount of energy absorption is almost identical in both cases.

Case C. The material is a cross ply laminate with the lamination planes in the vertical direction. In this case, the crack front is not straight as there are weak layers in the thickness where it can propagate easily. These weak layers let the crack surround the other layers and fracture the fibers without arresting the crack propagation. Thus we get a clean cut through the material, as can be seen in Fig. 16, without branching of cracks to the sides, and with a low level of energy absorption.

Case D. The material is a unidirectional laminate with the lamination planes in the vertical direction. Unlike all the other cases, here the failure occurs on the topside of the beams or the compression side. As the interlaminar surface is the weak link, the failure occurs by buckling and delamination between the layers, as can be seen in Figs. 16 and 17. This mechanism of failure occurs only here because at the bottom layer all the fibers are in the load direction, while in the cross ply material (vertical position) only half of the fibers are in the load direction and thus it is half as strong as the former case. In the horizontal position we do have delamination at the compression side as can be seen in Fig. 15, but it is restricted to a few layers while in

the vertical case it starts with many layers and propagates downward thus absorbing a large amount of energy.

4. Conclusions

This research study has thus far shown that fiber glass reinforced epoxies are rate sensitive when an impact load is applied on such materials. This fact must be considered when testing such materials. As a result, a common impact test, as the Charpy test, cannot give complete information since it supplies a constant amount of energy for different specimens some of which absorb most of the energy which is applied to them.

The higher strength and the higher energy associated with a high rate of loading is an advantage since it serves as safety factor for high rate loading. A deeper understanding of the mechanism of energy dissipation can lead to construction of materials to optimize the energy absorption.

As the mechanism of absorbing energy is delamination between layers and between fibers, the type of glass fiber does not change the material's toughness. The treatment which the fibers may have on their surface and the surface characteristics of the laminae, which control the delamination process, may change the ability of the material to absorb energy.

IV. CARBON FIBER COMPOSITES

1. Experimental Procedures and Results

The carbon fiber epoxy composites which were investigated were of two kinds and were fabricated by two different manufacturers.* The specimens were cut in the shape of rectangular bars from the plates supplied by the manufacturers. All the specimens were unidirectional, tested with the fibers along the length of the bars. Two types of fibers were used:

1. Hercules HMS (high modulus fibers)
2. Hercules HTS (high strength fibers)

The composite plates were made by Ferro Co.* with the epoxy E-293 (Ferro designation) as matrix ($\approx 35\%$ by weight) and some were made by Fiberite** with the epoxy X904 (Fiberite designation) as matrix for the high modulus fiber ($\approx 35\%$ by weight) and with the epoxy X05 (Fiberite designation) as matrix for the high strength fibers ($\approx 35\%$ by weight). The high strength material supplied by Ferro Co. was of two thicknesses. One plate was made with 25 layers and the other with 28 layers. Tests were performed on the Impact machine and on the high speed tension machine described earlier in the report. The quasi static values were taken from tests on an Instron testing machine, with velocities of 0.1 in/min for the crosshead. The flexural specimens were tested on three spans - 2", 3" and 4" using different impact velocities. For measuring the energy absorption, a special light weight tup was built from Lexan, because of the low energy absorption values of the carbon fiber composites. The fracture stress was measured also by applying the regular tup whose weight was 6.34 lb. The Lexan weight was only 0.936 lbs.

Fig. 20 shows the results of the fracture stress versus impact velocity for four different materials. As the thickness of the plates from which the specimens were cut was variable, the specimens are not all of the same thickness. Any point shown in Fig. 20 and on the subsequent figures are an average of at least 5 tests. It is seen that for the HTS fiber composites there is a slight increase in the fracture stress, while for the HMS fiber composites there is a slight decrease for increasing impact velocity. Manufacturer I identified in Fig. 20 is Fiberite Co. while Manufacturer II is Ferro Co. Where the manufacturer is not identified in other figures it was Ferro Co. Fig. 21 shows the influence of changing the span on the fracture stress.

* Ferro Corporation, Culver City, California

**Fiberite Corporation, Winona, Minnesota

As this is a high modulus and brittle material, the fracture initiates and propagates from the tension side of the bar. The failure starts when the combination of tension stress and shear stress reaches the failure stress for this material, which means that the failure stress depends on the span to thickness ratio as a change in failure mode may occur. The fracture was not an interlaminar shear fracture even at the smallest span shown; the calculated shear stress was much lower than the shear strength but the presence of the shear stress can influence crack initiation. Fig. 22 shows the failure tension stress as function of the span to thickness ratio. It is clearly seen that the strength depended on this ratio, and even the data for the materials from different manufacturers agrees well. Tests were performed on a high speed tension machine to compare the behavior with the impact machine and also to control the deflection rate. Fig. 23 shows some oscilloscope records taken from the high speed tension machine and from the impact apparatus. Both records show the same load-time curve, which is linear, and hence the deflection is linear with time, when performing drop weight impact tests as it is on the high speed tension machine. Fig. 24 shows the results from the high speed tension machine along with some results from the impact tests. It is seen that there is good agreement between these results for different spans and impact velocities. There is a slight increase in the strength for both the HTS material and the HMS material. Fig. 25 shows oscilloscope records for the HMS material tested on the high speed tension machine as well as from the impact apparatus. The load-time curve from the high speed tension machine has an initial region of non-linear loading compared to the impact. This is a result of the machine stiffness. The strength results are very similar from both machines. For studying the mechanism of fracture and energy absorption, a high speed camera was used while impacting the specimen. The failure mode was found to be crack initiation from the tension side of the specimen followed by propagation through the cross section with considerable

pull-out of fibers. Fig. 26 shows a series of pictures taken from the high speed movie showing the crack growth. The material contains the HMS carbon fibers, and the time interval between each frame is 0.16 ms. The crack started at the bottom tension side of the beam as seen at the top picture and propagated to the upper compression side of the beam. Because of the acceleration given to the specimen by the drop weight, the specimen moves faster than the weight tip after fracture as seen on the other pictures. The mechanism of the fracture is not a smooth crack propagation through the cross section, but it involved pull-out of fibers from both sides of the cross section. This is seen clearly on the series of pictures in Fig. 27 for both the HMS fiber composites and the HTS fiber composites. Fiber pull-out occurs for both types of materials. The energy which was absorbed by the fracture of the specimens during the impact loading for the 2" span is shown in Fig. 28. The zero velocity values were measured as the area under the stress-strain curve from a test performed on an Instron machine. Since the thickness of the specimen varied, the data was first plotted with the fracture energy divided by the cross section area. It was concluded that the cross section area was not a parameter which could normalize the results, or in other words the energy absorbed is not a linear function of the thickness (as it is a linear function of the width). The energy absorption as a function of load rate for a 3" span and 4" span is plotted in Fig. 29. It appears that the HMS fiber composites are not sensitive to the rate of loading while the HTS fiber composites have some dependence on the rate. In Fig. 30, the average fracture energy (from Figs. 28 and 29) is plotted as a function of the span and also compared with the elastic energy which was stored in the material just before it failed. The calculation of the elastic stored energy is based on the applied load during impact and the modulus of elasticity measured from the high speed tension machine. We can see that the energy absorbed is linearly related only to the width of the specimen, and it is not a simple function of the other dimensions or a relation between them, and

therefore of course it is not related to the elastic energy stored in the material just before failure.

2. Conclusions

Further work must be done with the carbon fiber composites to elucidate the failure mechanism. The high speed photography must be improved so that a greater number of frames/second is achieved due to the rapid crack propagation through the specimen. The results thus far indicate only a slight increase in strength with loading rate, contrary to the glass fiber composites. The energy absorption increase with increasing loading rate is also not as great as for some glass fiber reinforced plastics. Also, the calculated value of elastic strain energy absorbed for carbon fiber composites is much nearer the measured value of energy absorption than for glass fiber composites. At this time, it is clear that energy absorption is not simply related to most experimental variables and the results of standard tests such as the Charpy test should be interpreted carefully when trying to relate them to real problems.

REFERENCES

1. Broutman, L. J. and Krock, R. H., "Modern Composite Materials", Addison-Wesley Publishing Co., Reading, Massachusetts 1967.
2. Outwater, J. O. and Murphy, M. C., 24th Annual Technical Conference Reinforced Plastics/Composites Division, S.P.I. Sec. 11-C (1969).
3. Piggott, M. R., J. Materials Science, 5, (1970), pp. 669-675.
4. Tetelman, A. S., "Composite Materials, Testing and Design" ASTM, STP, (1969), p. 460.
5. McGarry, F. S. and Mandell, J. F., MIT Research Report R70-79 (Dec. 1970).
6. Impact Testing of Metals, ASTM Special Technical Publication (1970), p. 466.
7. Revsin B. and Bodner, S. R., Israel Journal of Tech., Vol. 7, No. 6, (1969) p. 485.
8. Novak, R. C. and De Crescente, M. A., Second Conference on Composite Materials Testing and Design, ASTM, April 1971.
9. Barker, A. J., "Charpy Notched Impact Strength of Carbon-Fibrex Epoxy-Resin Composites," The International Carbon Fibres Conference and Exhibition, The Plastics Institute, London, 1971.
10. Sidney, G. R. and Bradshaw, F. J., "Some Investigations on Carbon-Fibre Reinforced Plastics under Impact Loading and Measurement of Fracture Energies".
11. Rotem, A. and Lifshitz, J. M., 26th Annual Tech. Conference RPD/SPI, 10-G, (1971).

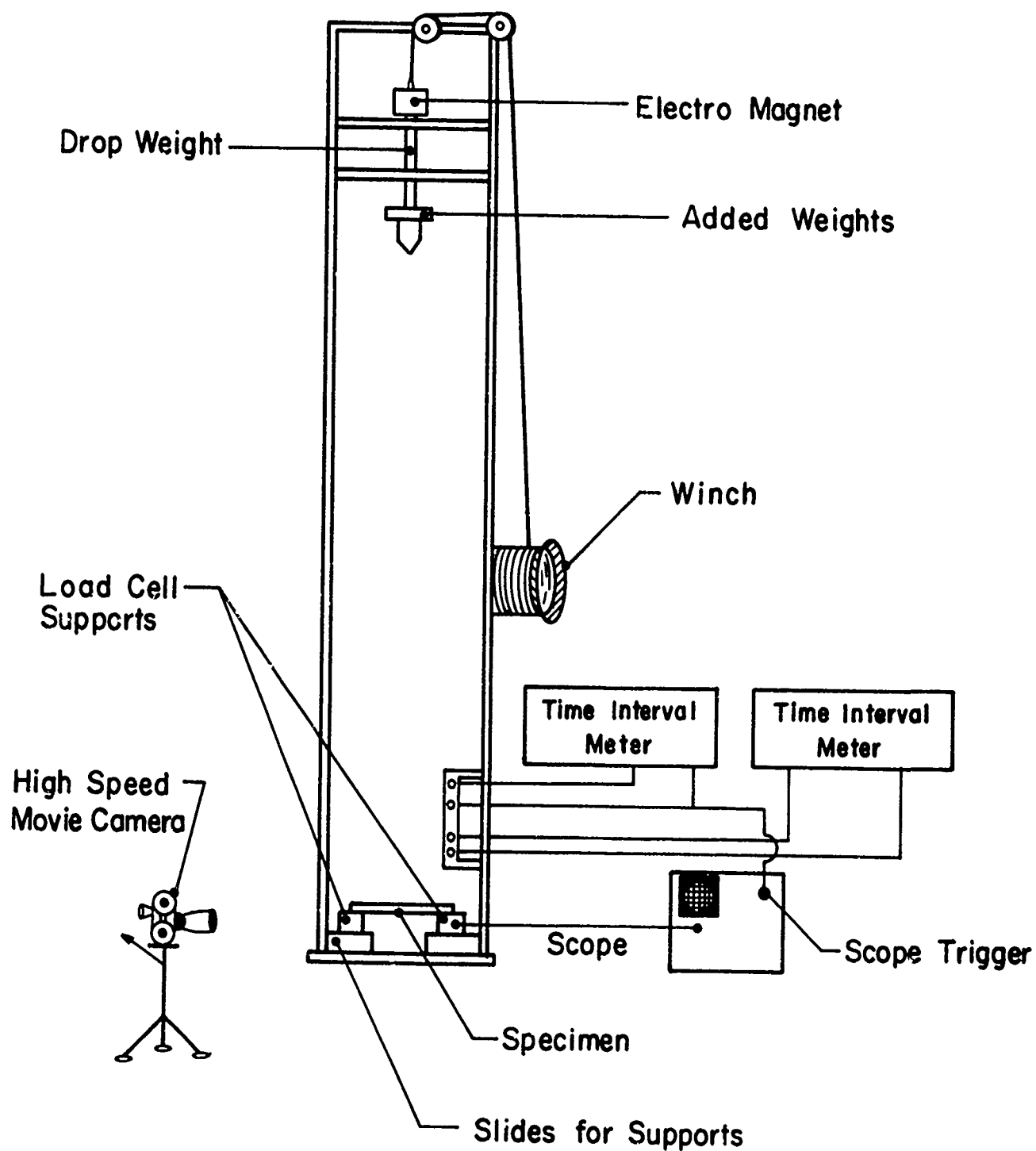


Figure 1 Schematic Diagram of Drop Weight Impact Apparatus



Figure 2 View of Drop Weight Impact Apparatus

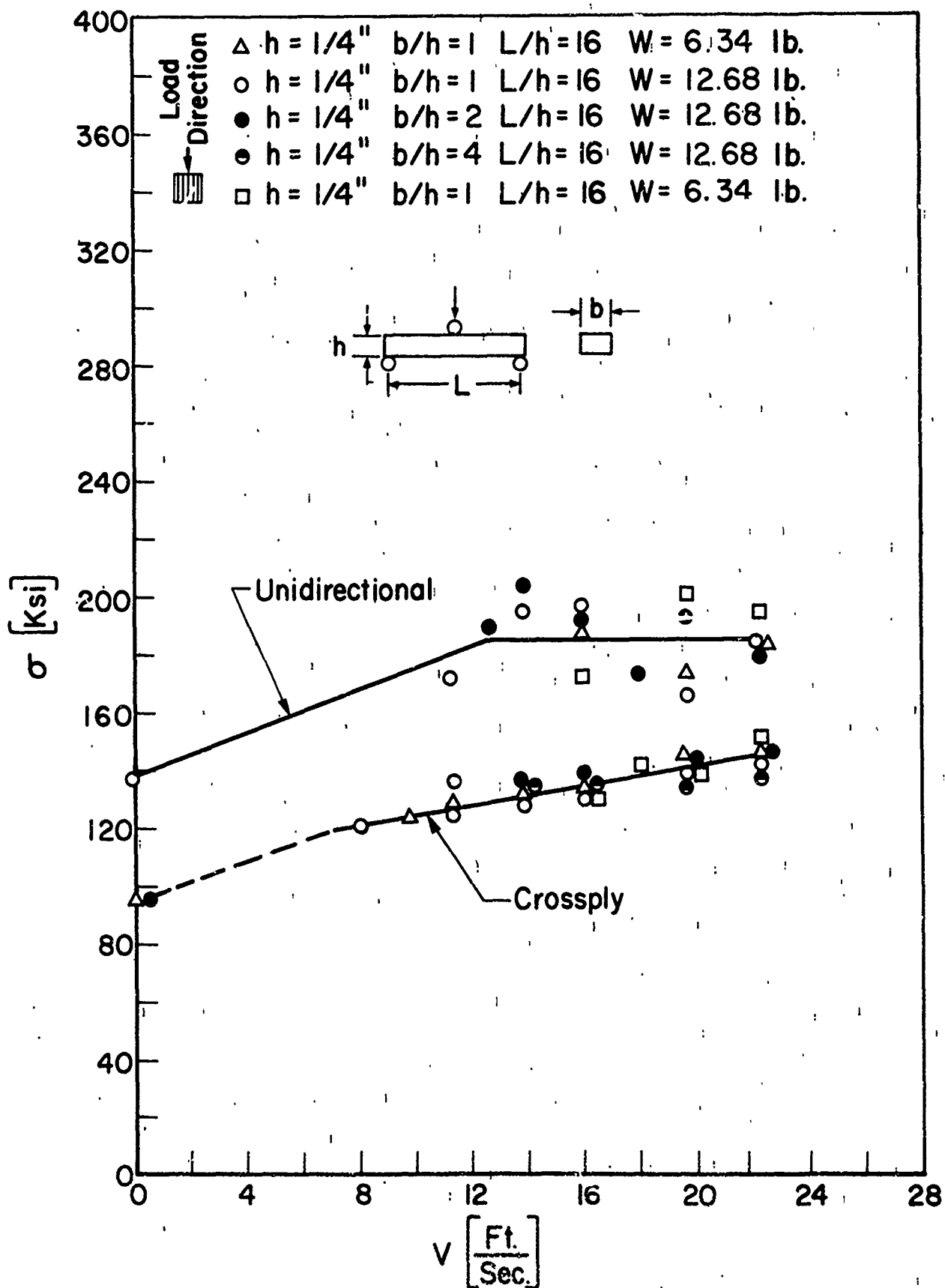


Figure 3 Strength of E-Glass Laminates as a Function of Loading Rate

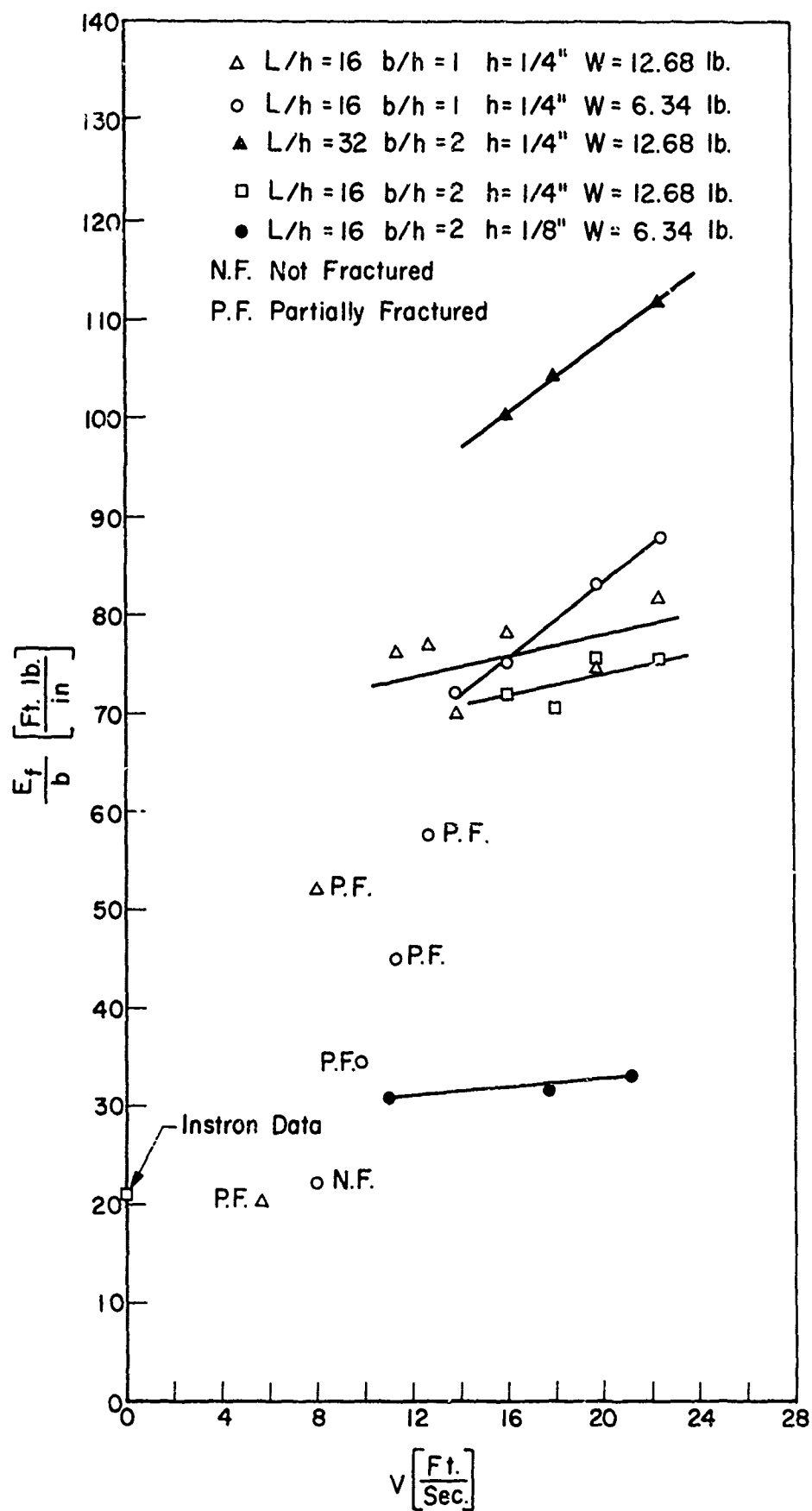


Figure 4 Energy Absorption of E-Glass Laminates (Cross-ply) as a Function of Loading Rate

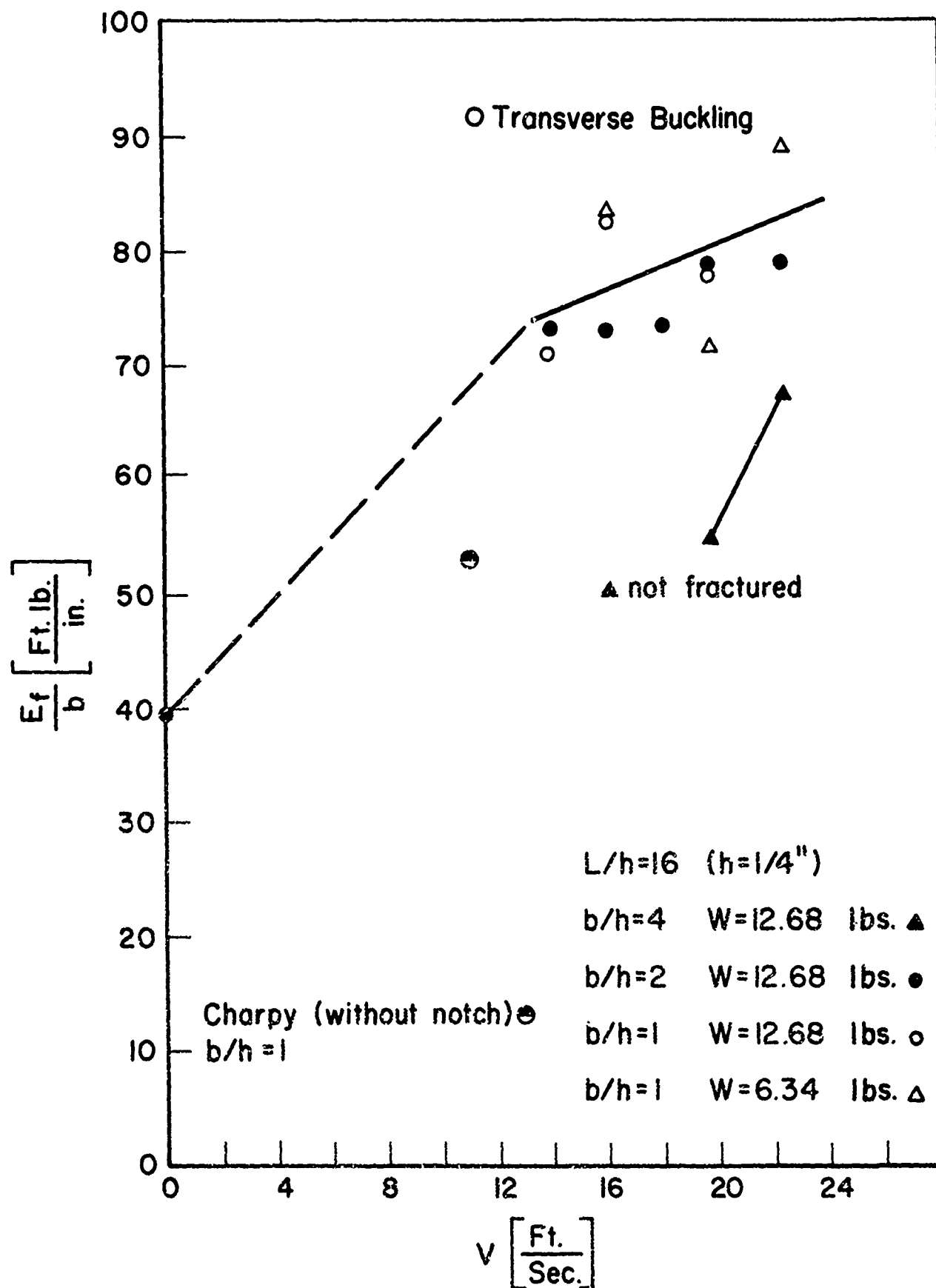


Figure 5 Energy Absorption of E-Glass Laminates (Unidirectional) as a Function of Loading Rate 25

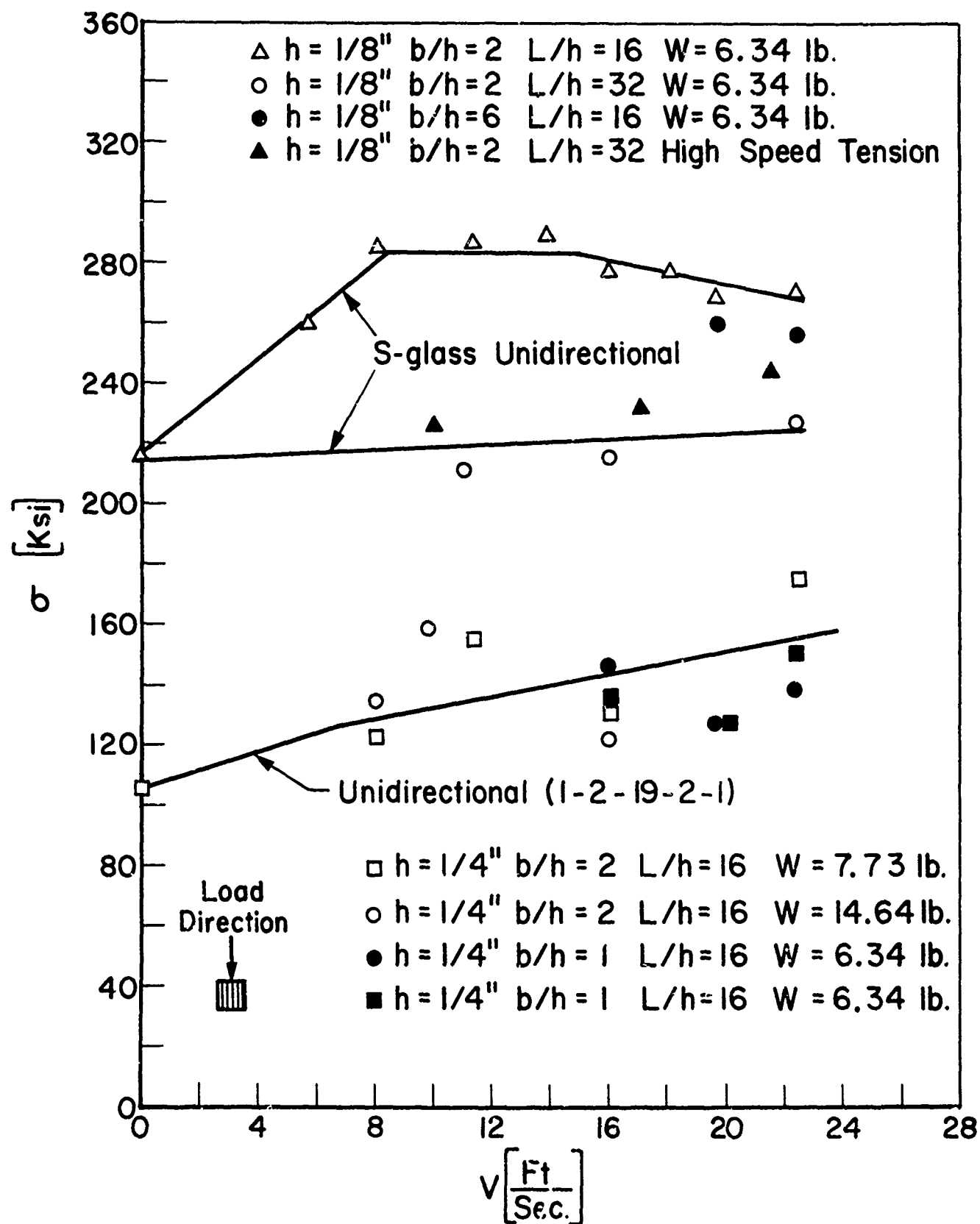


Figure 6 Strength of E-Glass and S-Glass Laminates (Unidirectional) as a Function of Loading Rate

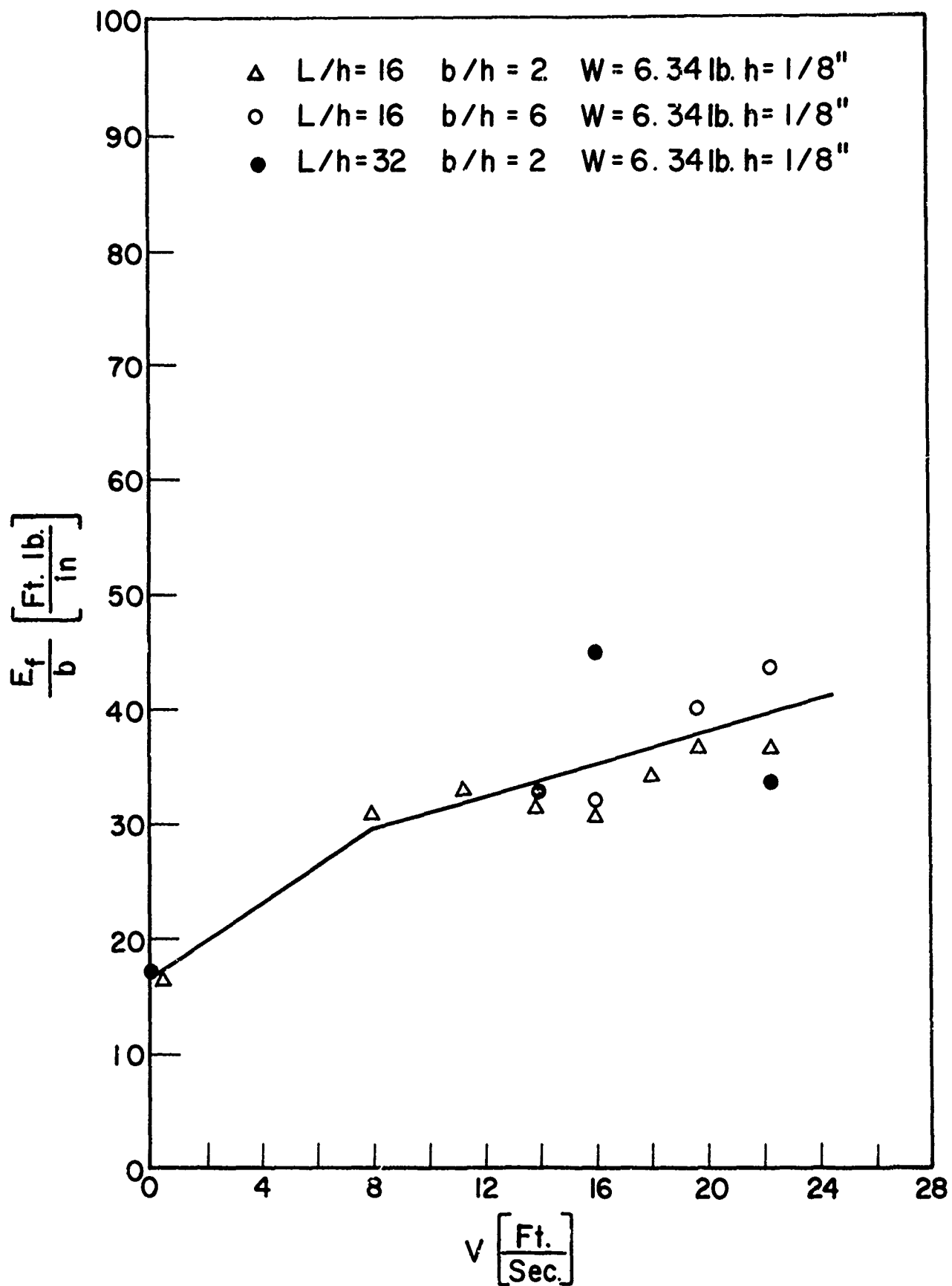


Figure 7 Energy Absorption of S-Glass Laminate (Unidirectional) as a Function of Loading Rate



The Effect of the Lamination Plane Orientation on the Energy Absorption of E-Glass Laminates

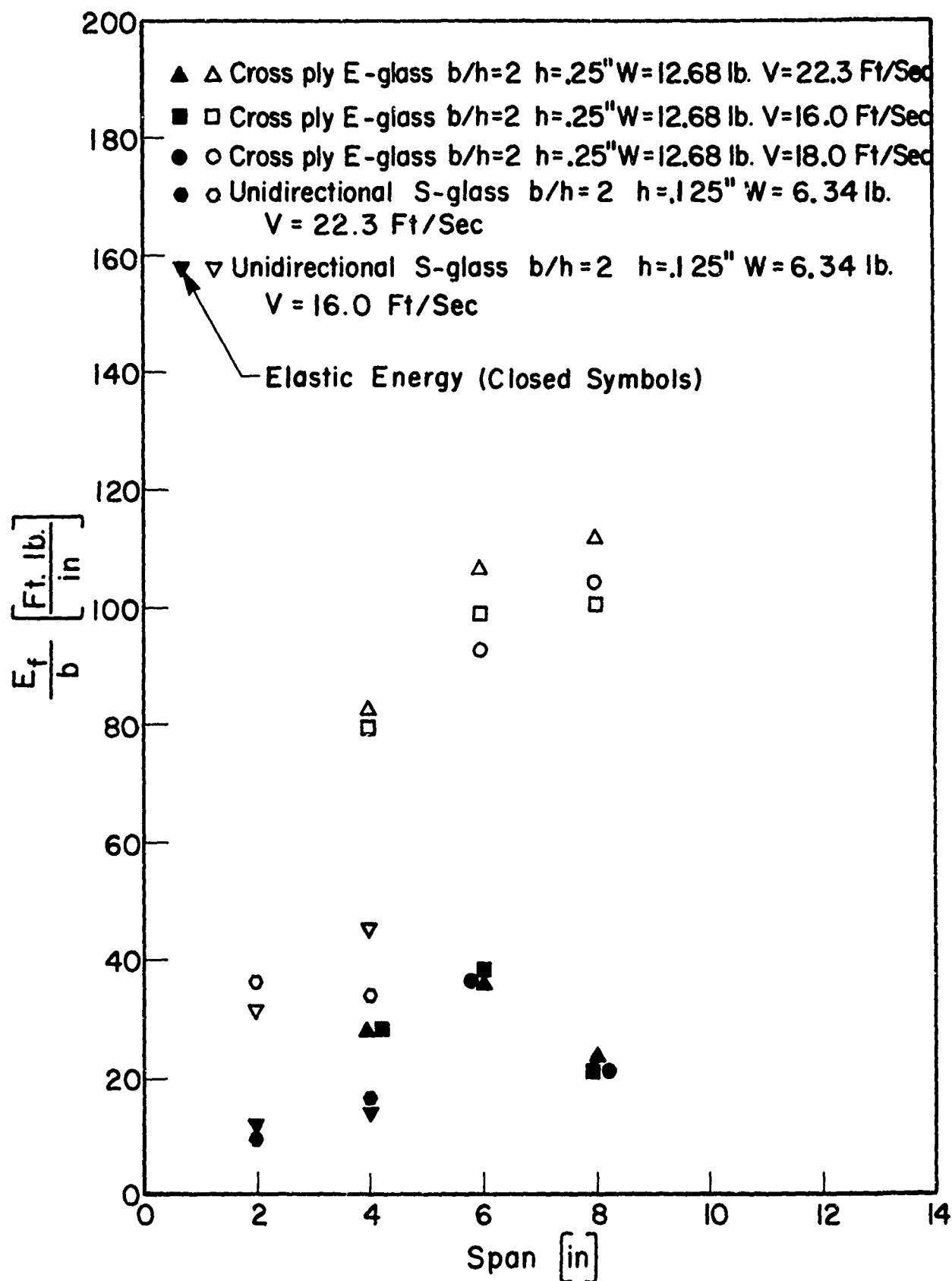


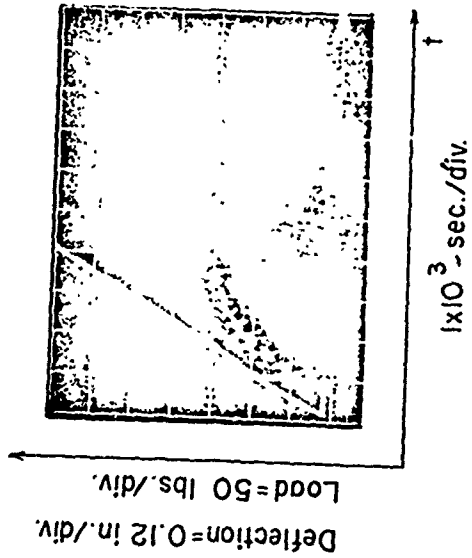
Figure 9

27
 Energy Absorption of E-Glass and S-Glass Laminates as a Function of Beam Span

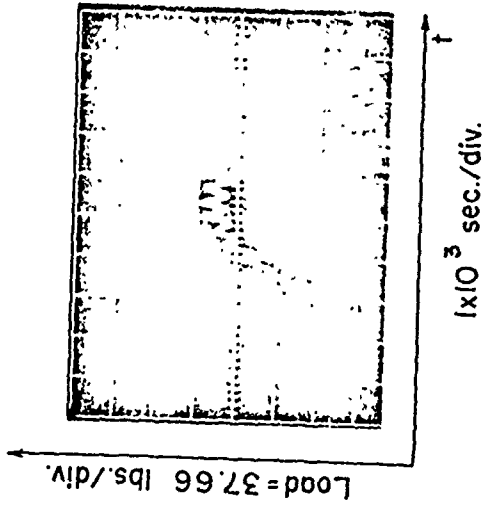
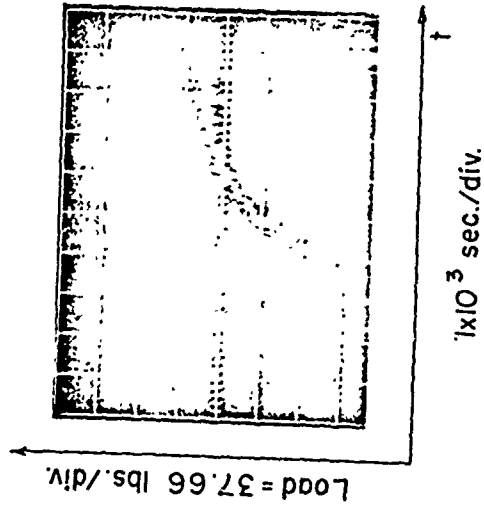
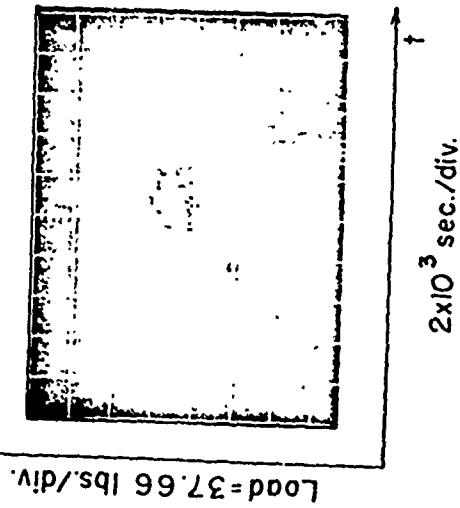
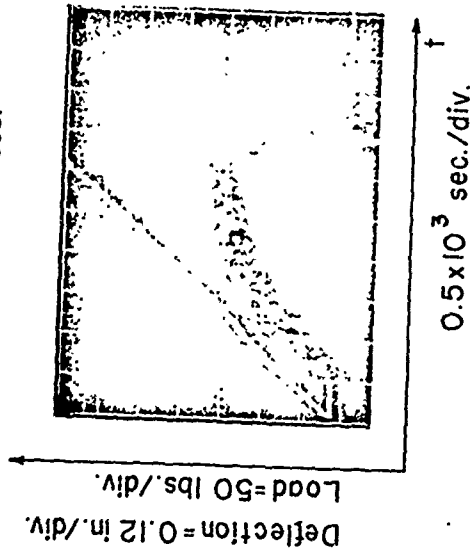
V=10 ft./sec.



V=17 ft./sec.



V=21.5 ft./sec.



28

Figure 10 Oscilloscope Records of Load and Deflection for S-Glass Laminates Tested in Bending (4 inch span). Upper Records from High Speed Testing Machine, Lower Records from Drop Weight Impact Apparatus

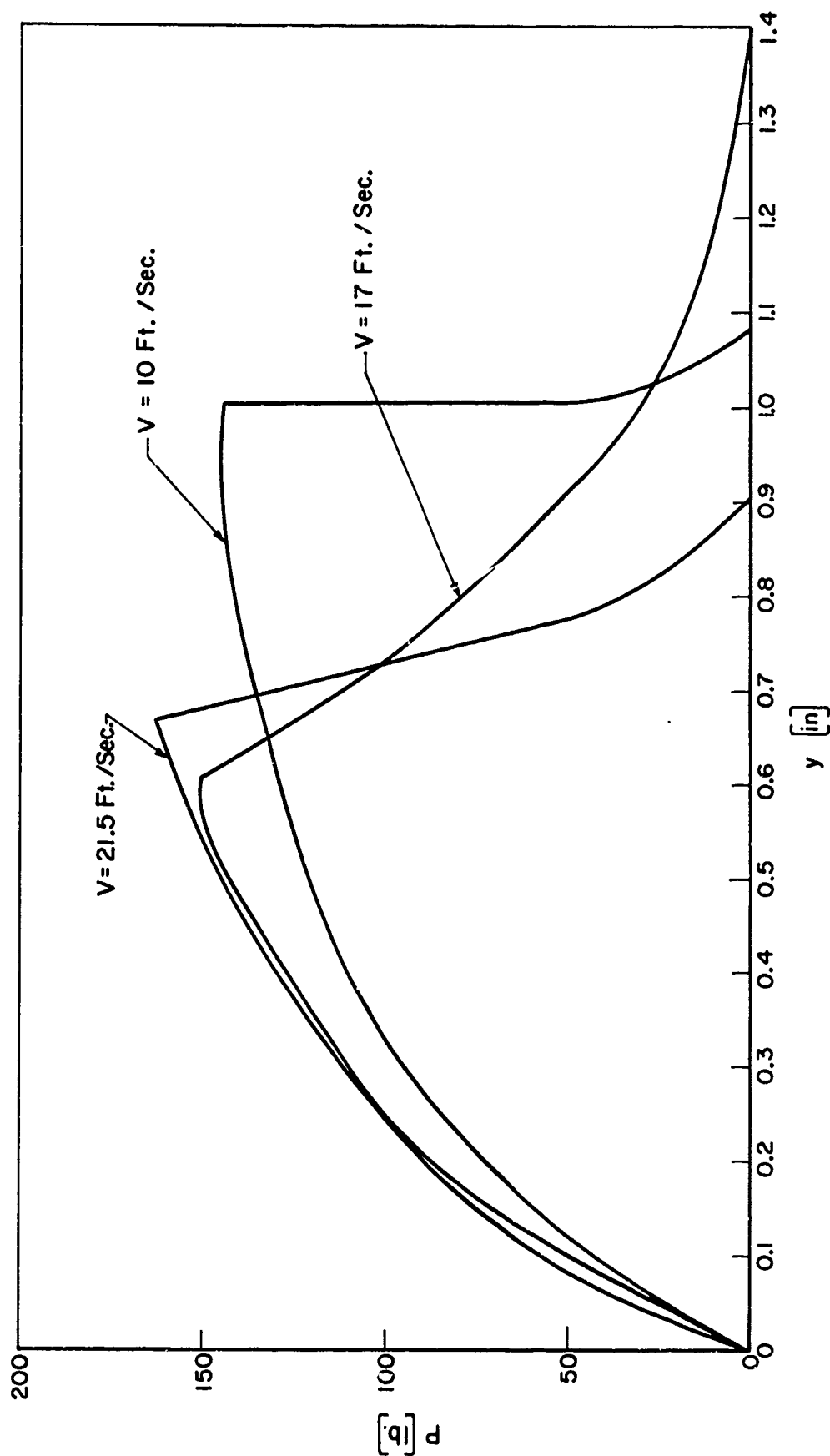


Figure 11 Load-Deflection Curves for S-Glass Laminates in Bending. Results Taken from Oscilloscope Records in Figure 10

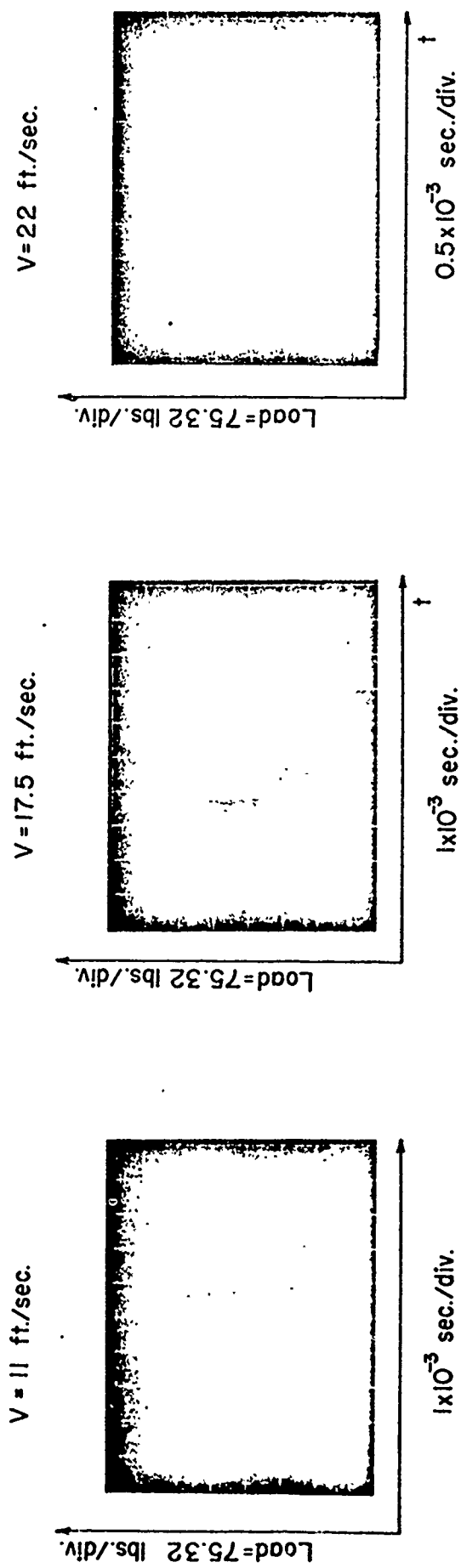


Figure 12 Oscilloscope Records of Load and Deflection for S-Glass Laminates Tested in Bending (2 inch span).

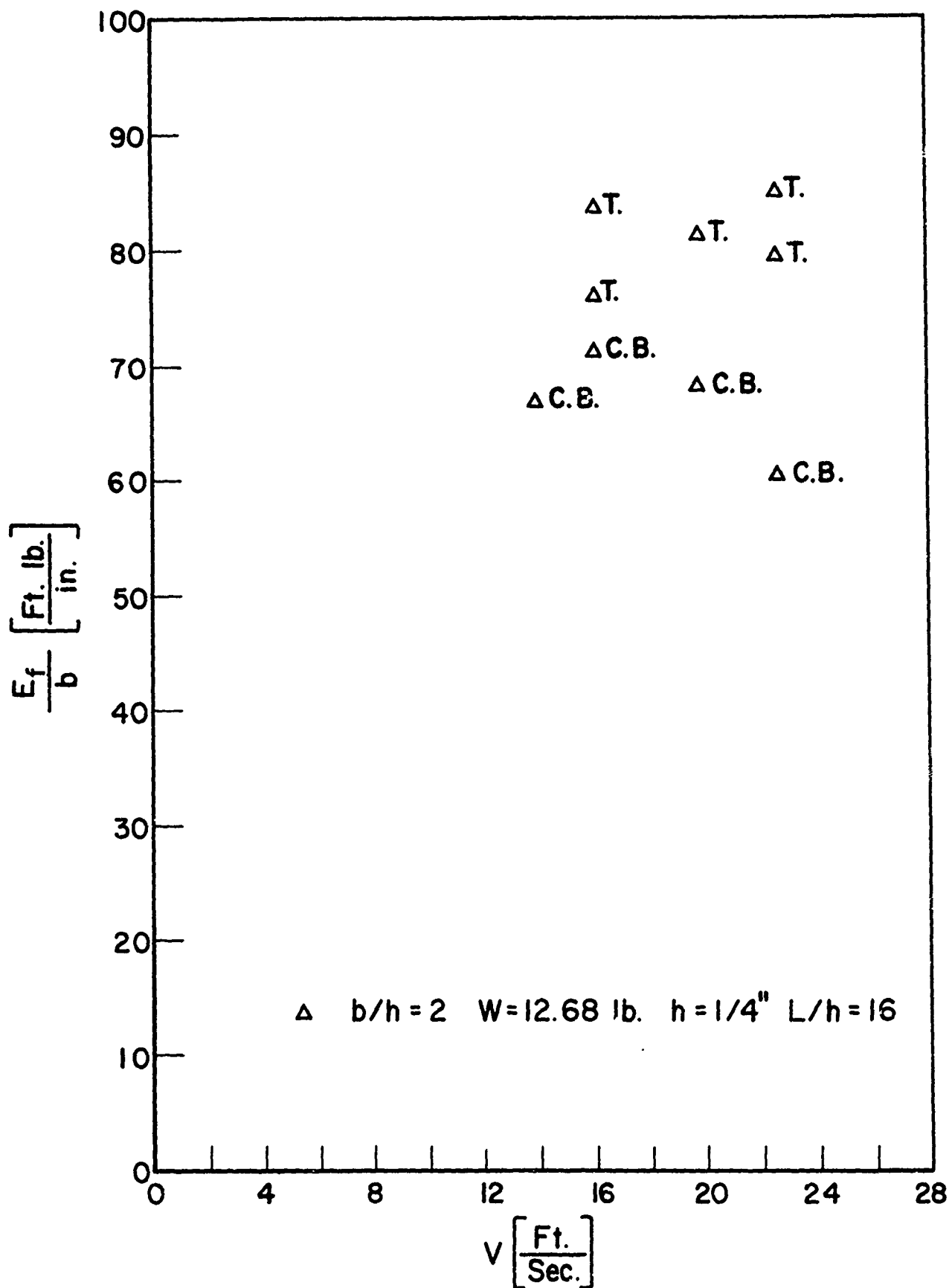


Figure 13

The Effect of Failure Mode on Energy Absorption E-Glass Cross-ply Laminates

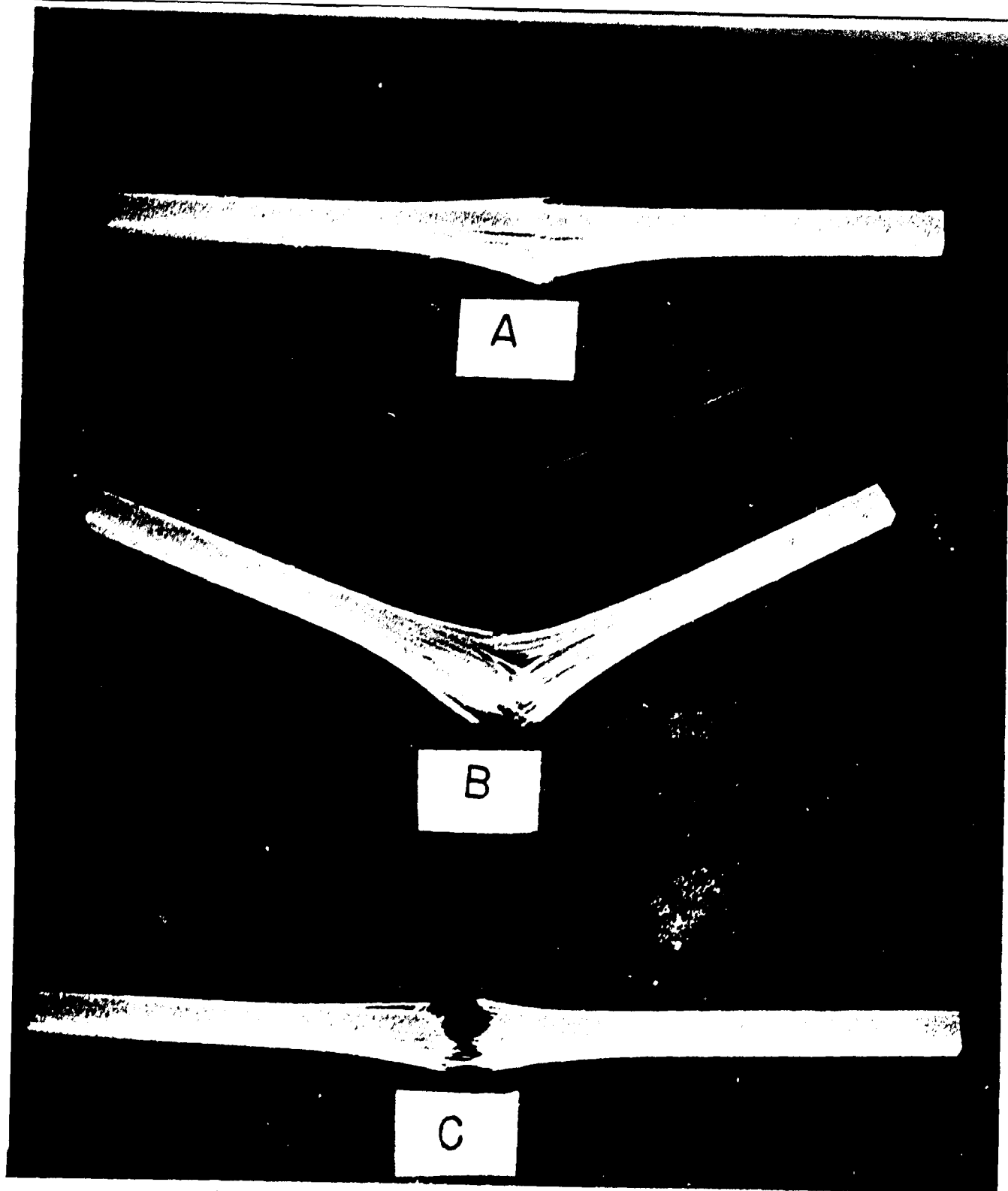


Figure 14

Fracture Modes of E-Glass Cross-ply Laminates. A: Partially Failed Specimen with Tensile Fracture. B: Tensile (T) Fracture. C: Cut (C.B.) Type of Fracture

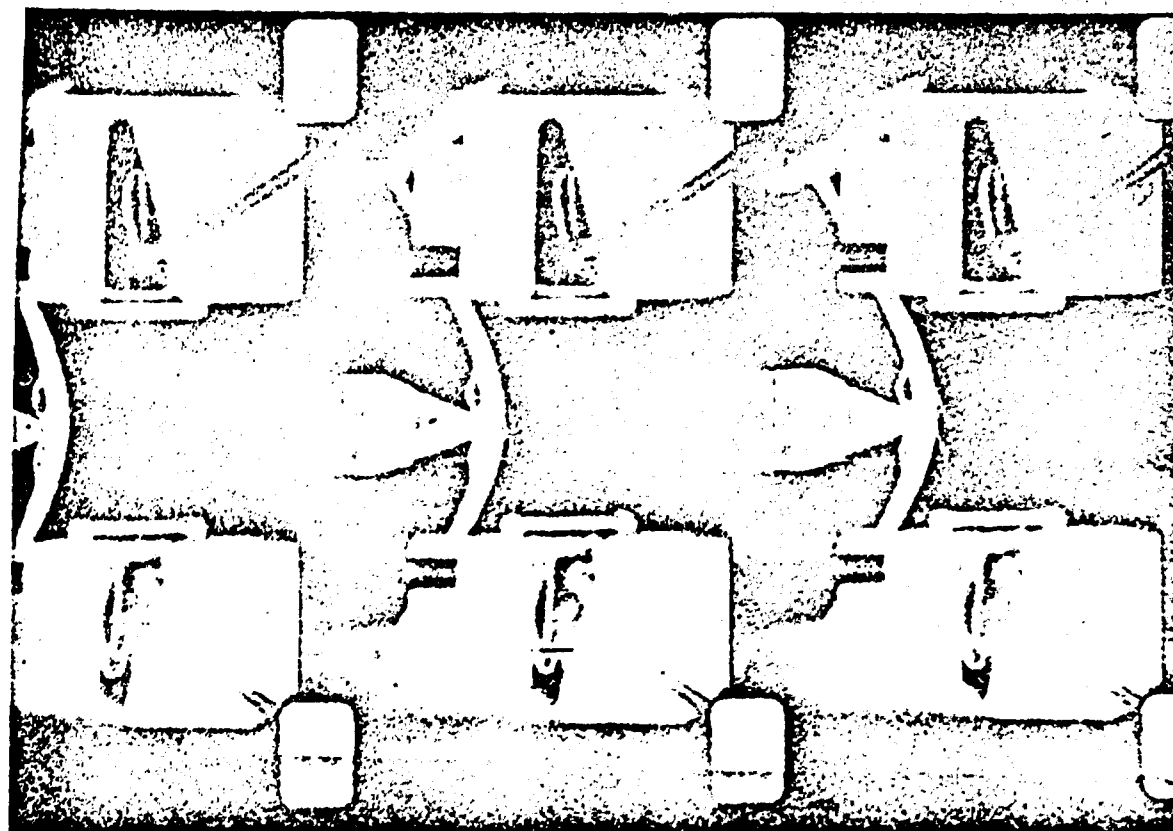
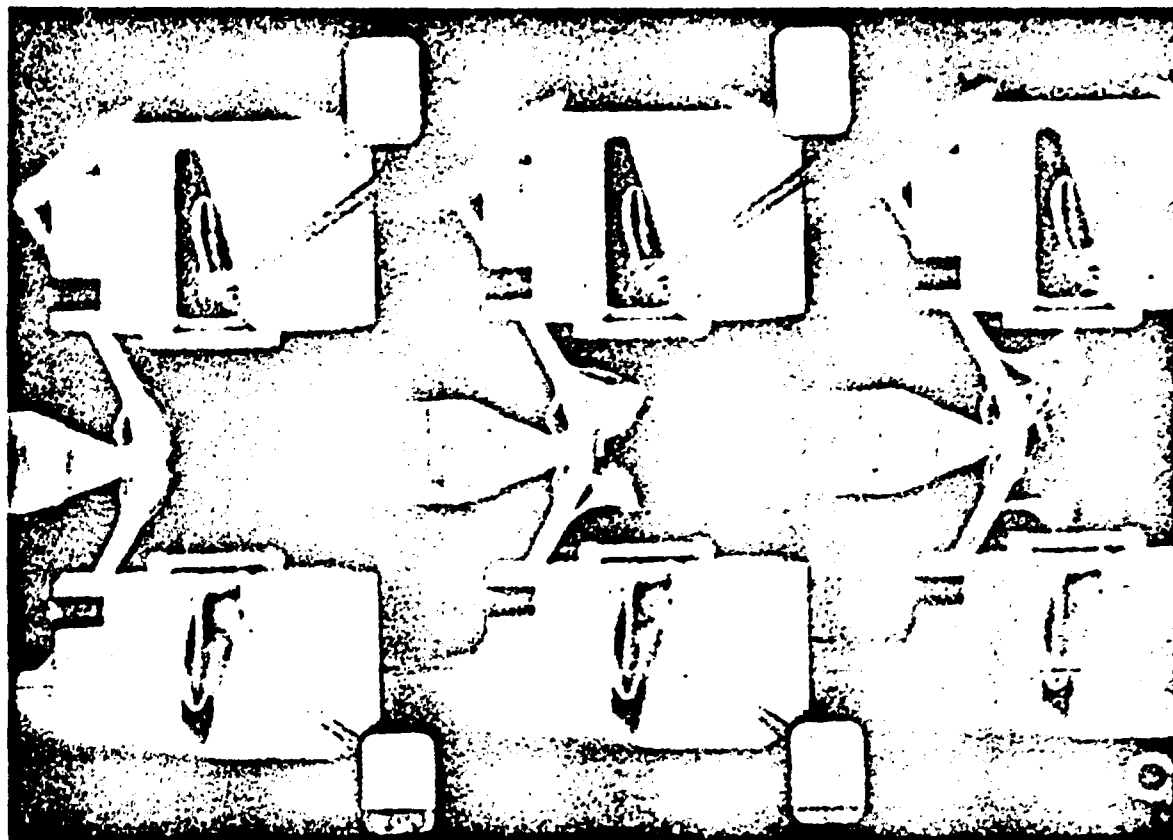


Figure 15

Frames from High Speed Movie of Tensile (T) Fracture in E-Glass Cross-ply Laminate. Frame begins at upper right hand corner and continues down. Fourth frame is at upper left hand corner.

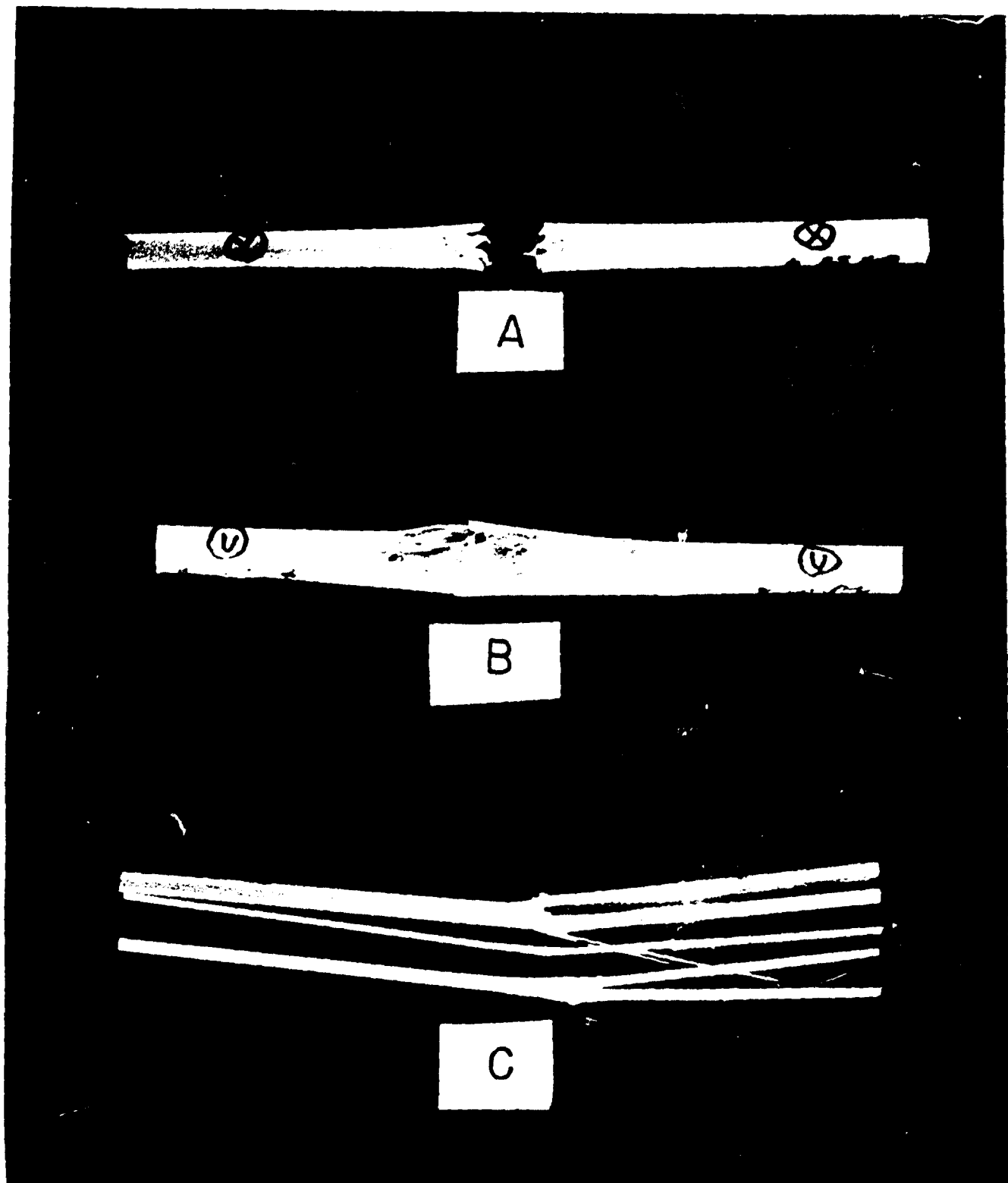
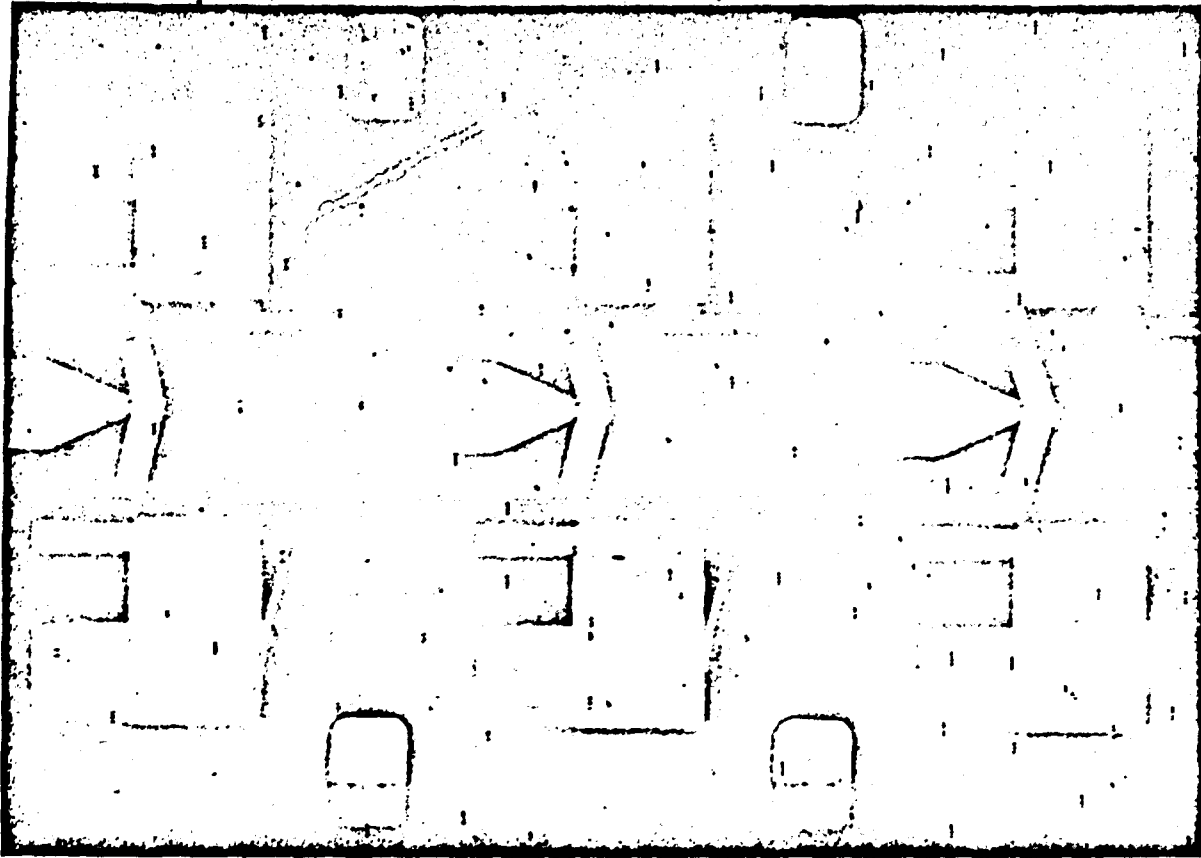
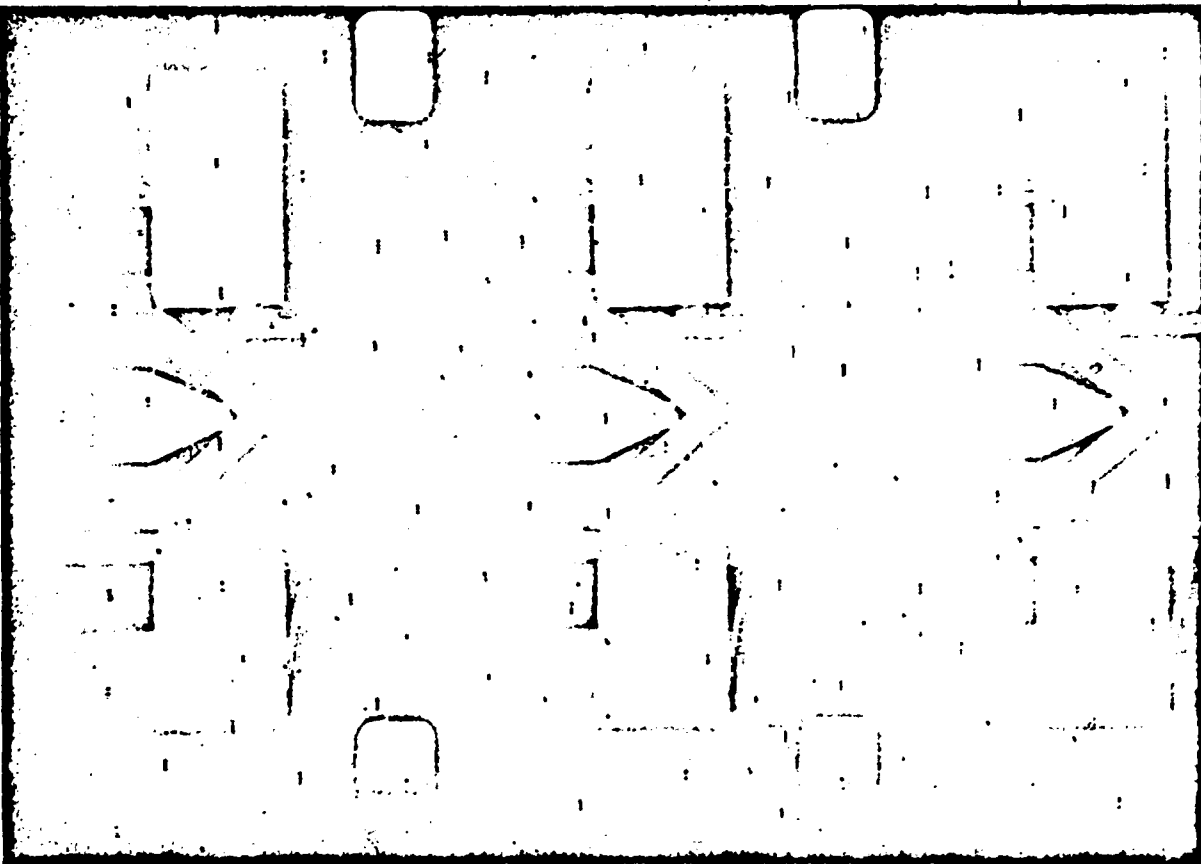


Figure 16

Fracture Modes when the Laminate is Impacted so that the Lamination Planes are Vertical. Photograph shows top surface or impacted surface.

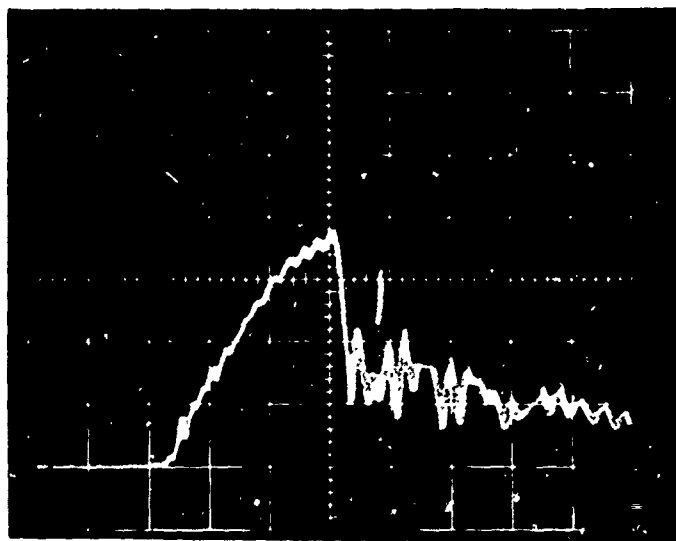
- A. Shear mode of fracture in E-Glass cross-ply laminate
- B. Transverse buckling mode of fracture in unidirectional laminate
- C. Delamination mode of fracture in unidirectional laminate

24



Frames from High Speed Movie of Transverse Buckling Fracture in E-Glass Unidirectional Laminates. Frame begins at upper right hand corner and continues down. Fourth frame is at upper left hand corner.

Figure 17

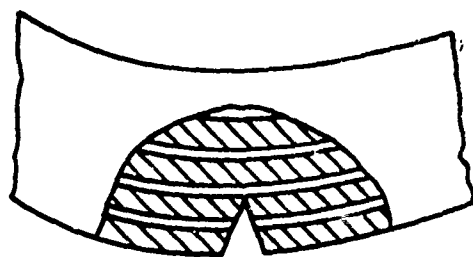


CROSS PLY E GLASS / EPOXY

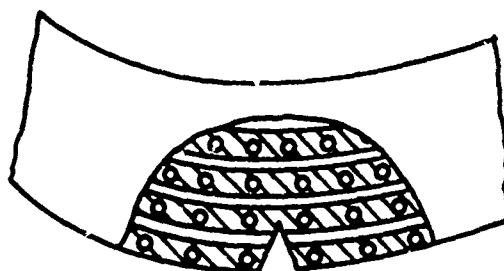
$h=1/4"$ $L/h=16$ $b/h=2$ $v=18\text{ft/sec}$

Figure 18

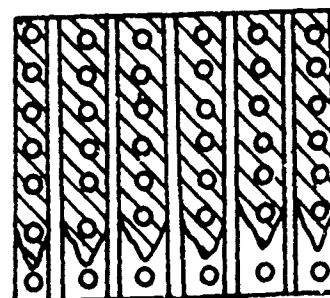
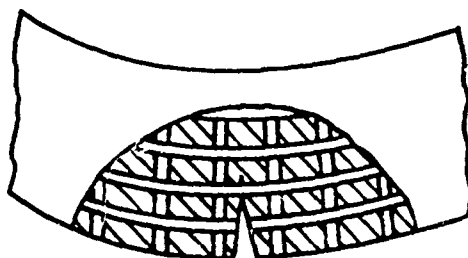
Oscilloscope Record for Case when Applied Energy is only Slightly Greater than that Needed to Fail Specimen



CASE A



CASE B



CASE C

Figure 19 Suggested Failure Modes for Unidirectional and Cross-ply Laminates

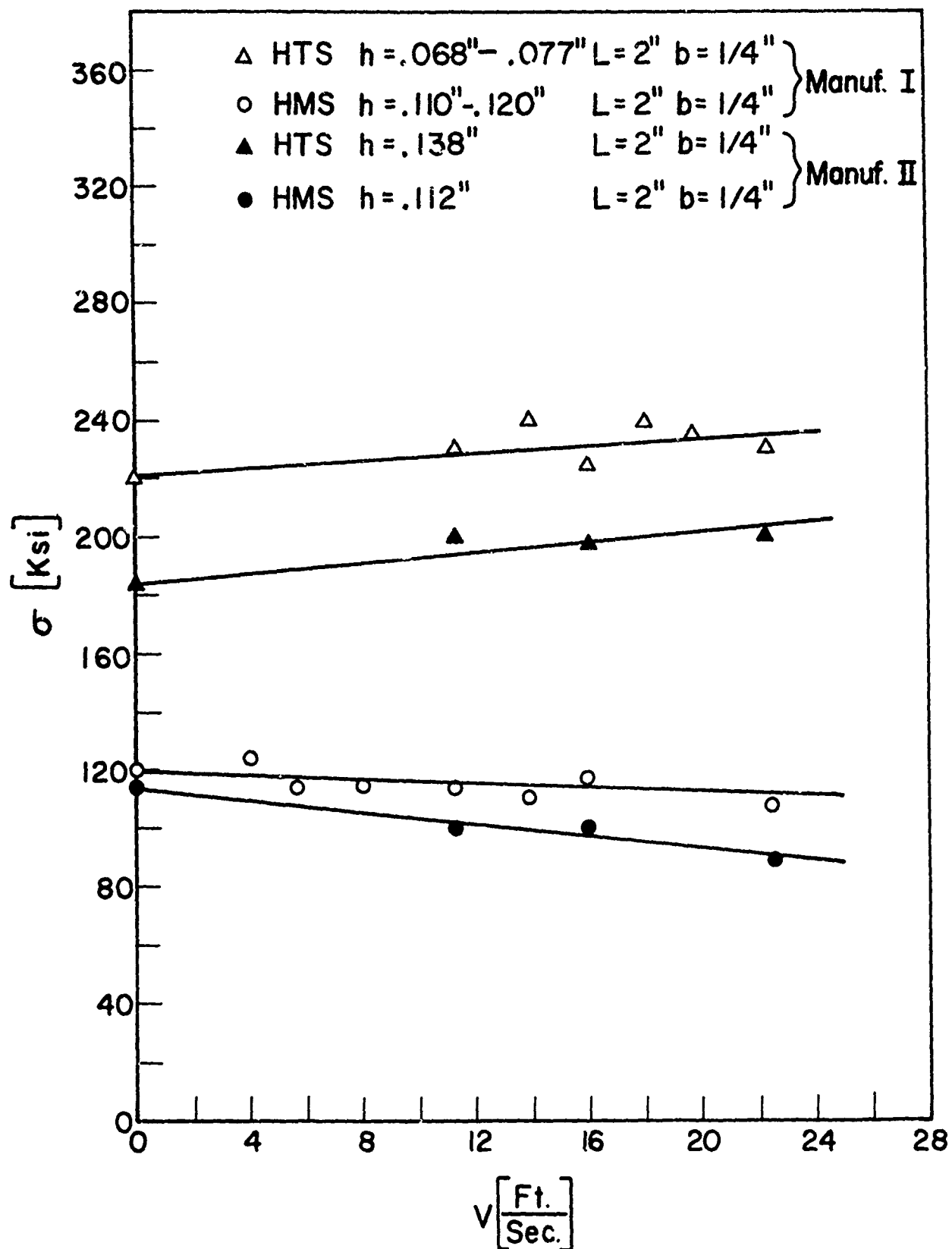


Figure 20

Strength of Carbon Fiber Composites as a Function of Loading Rate

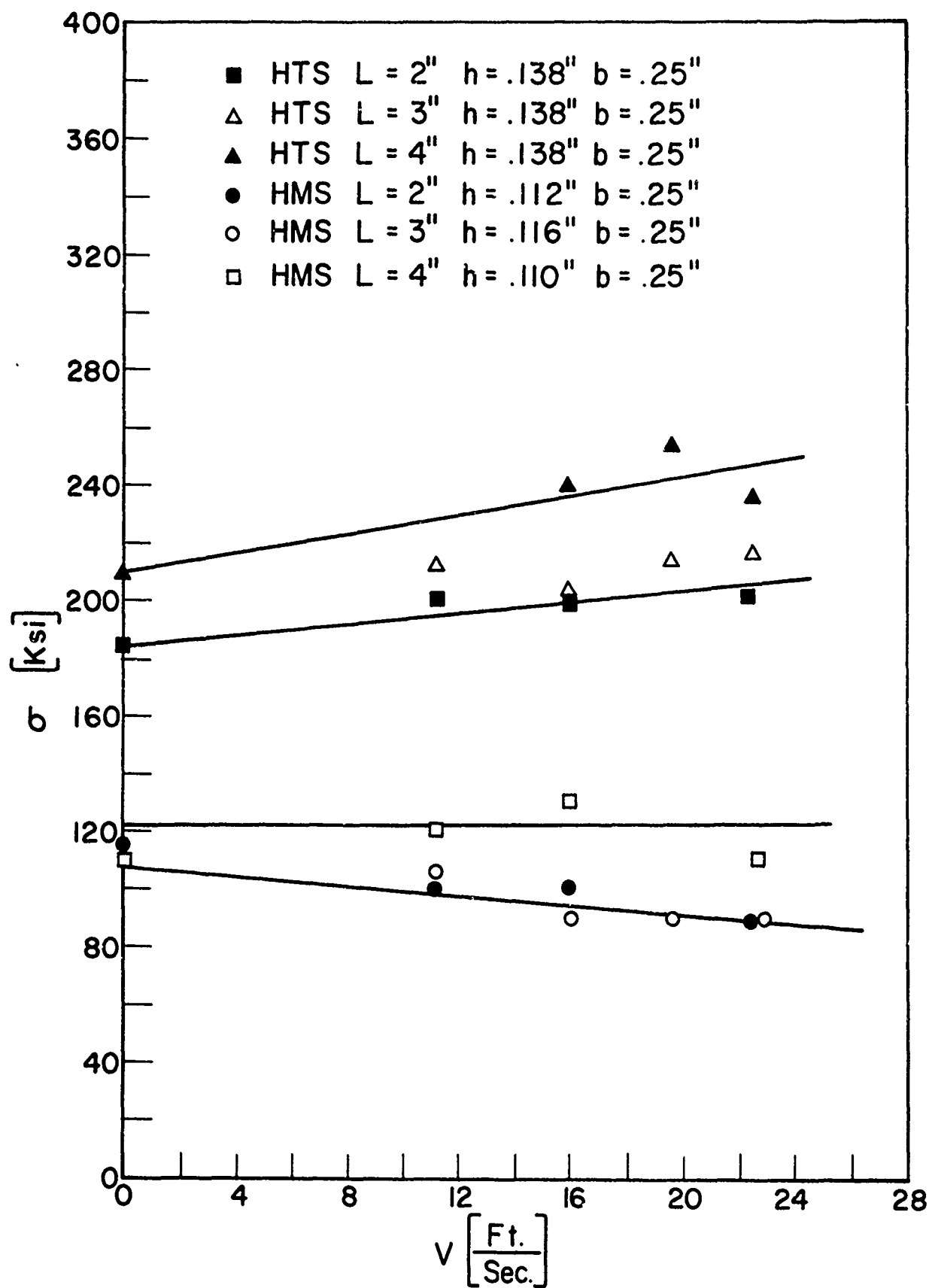
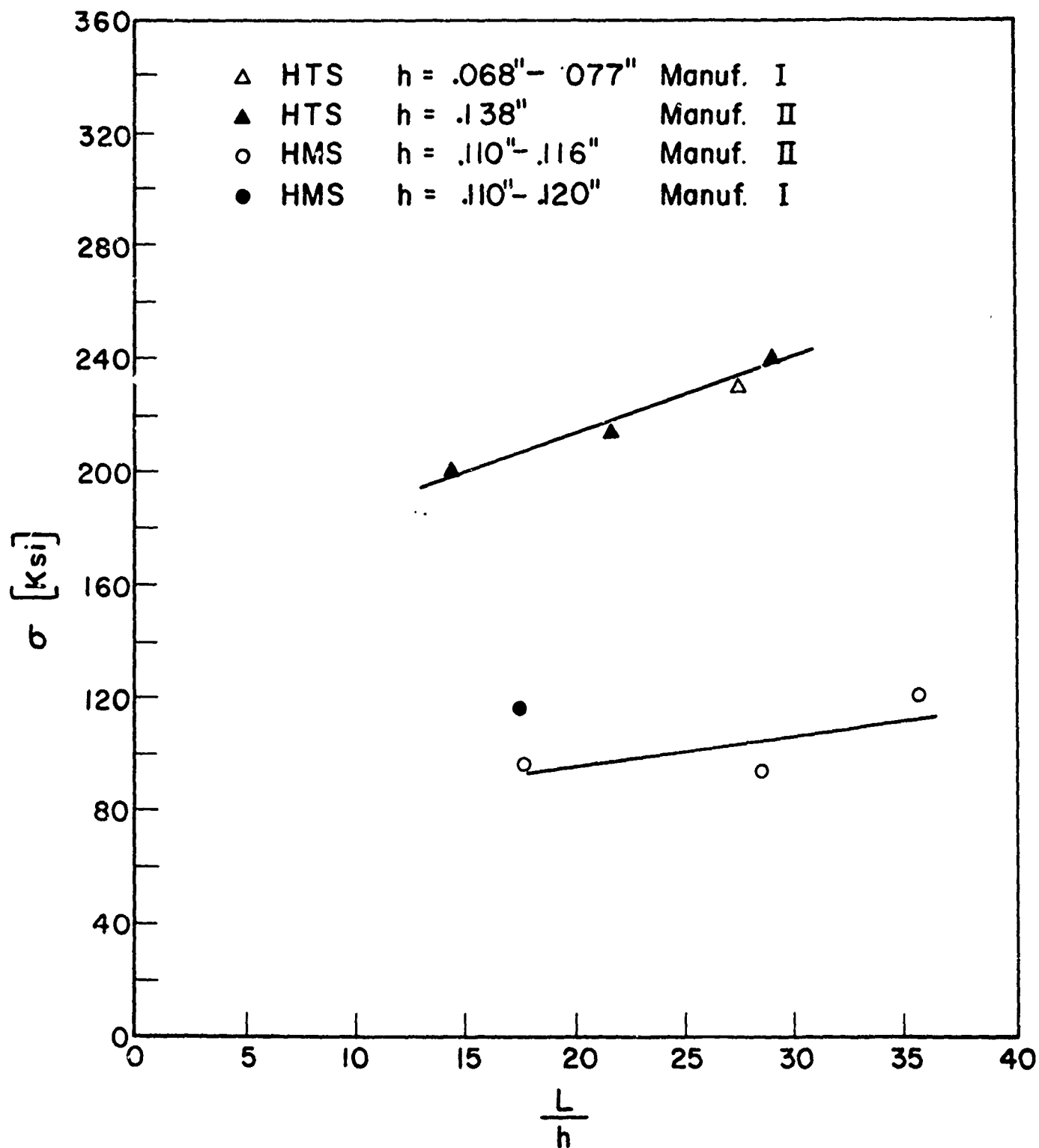


Figure 21

The Effect of Beam Span and Loading Rate in the Strength of Carbon Fiber Composites



40

Figure 22

The Effect of Beam Span to Depth Ratio on Strength of Carbon Fiber Composites

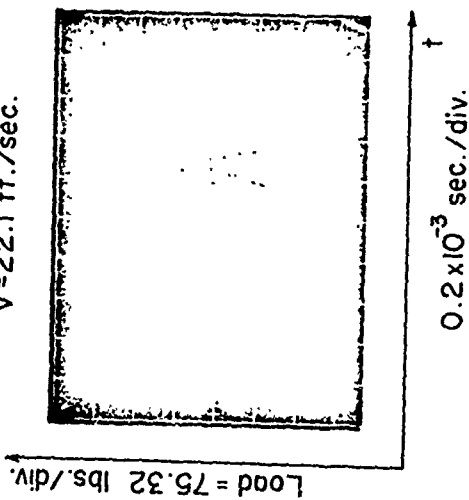
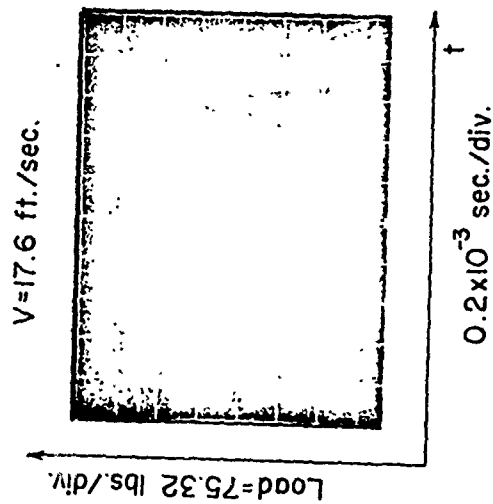
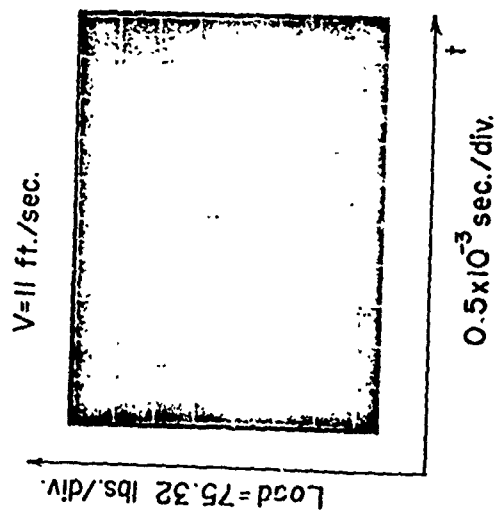
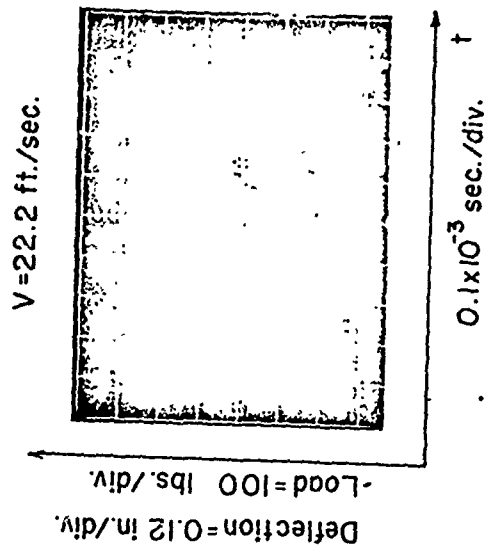
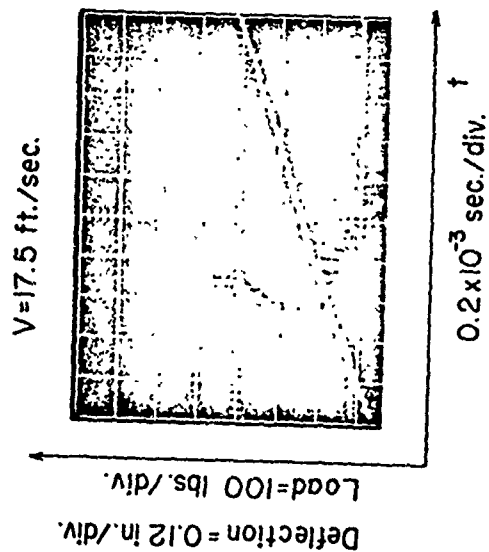
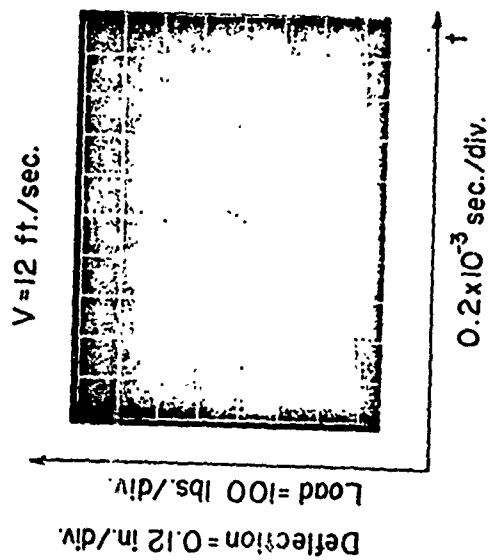


Figure 23

Oscilloscope Records of Load and Deflection for HTS Fiber Composites with 2 inch Beam Span. Upper records from high speed tension machine and lower records from drop weight impact apparatus

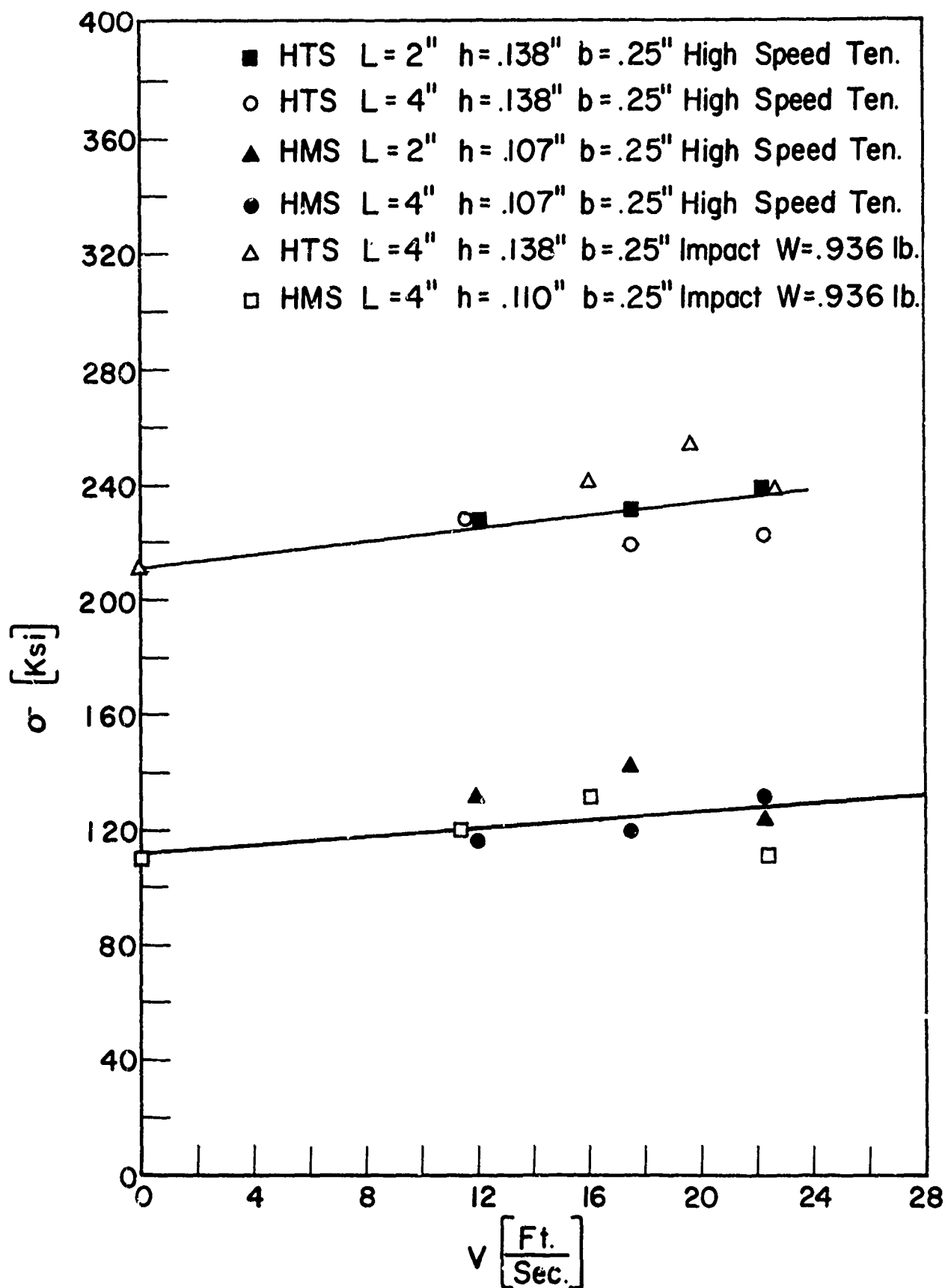
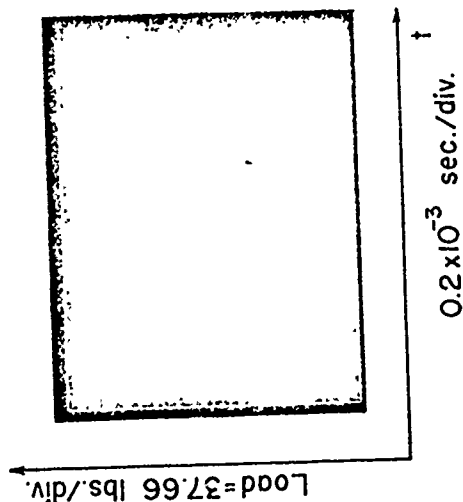
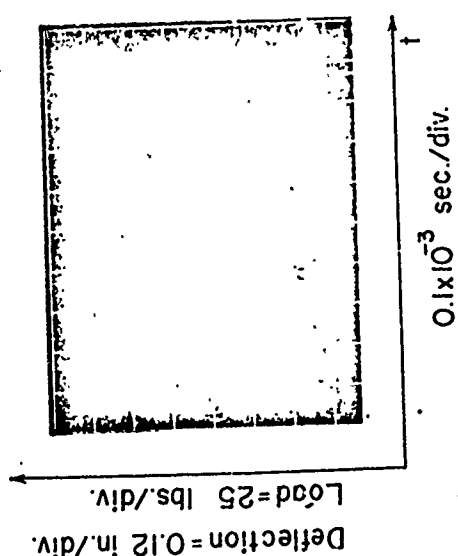


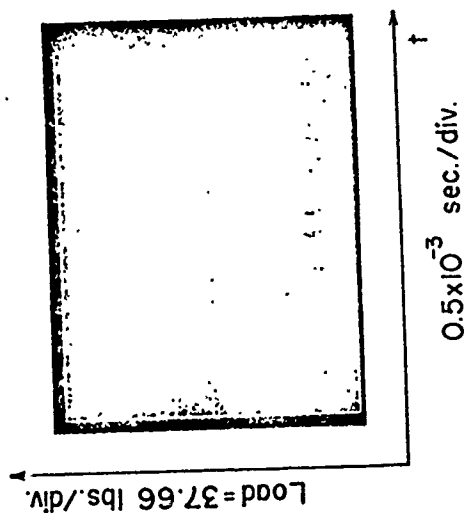
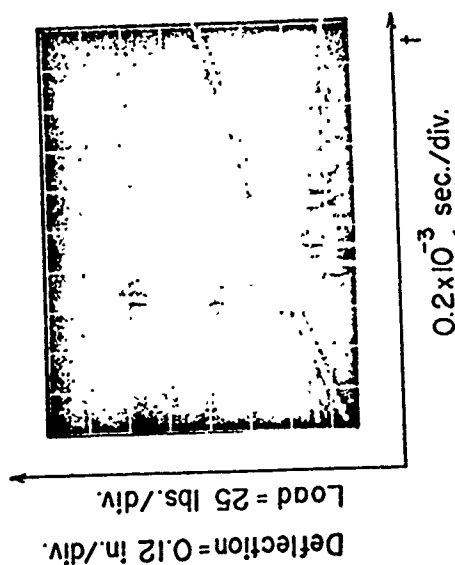
Figure 24

Strength of Carbon Fiber Composites Determined from High Speed Tension Machine and Drop Weight Impact Apparatus

V=22 ft./sec.



V=17.5 ft./sec.



V=11 ft./sec.

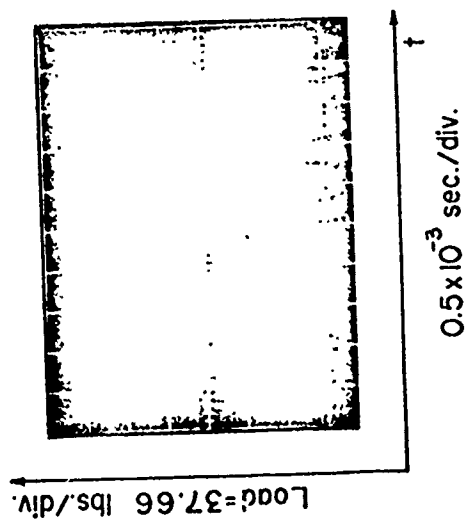
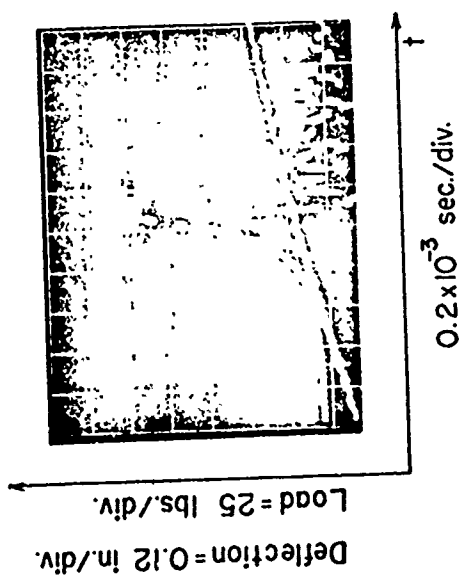


Figure 25 Oscilloscope Records of Load and Deflection for HMS Fiber Composites with 2-Inch Beam Span. Upper records from high speed tension machine and lower records from drop weight impact apparatus

Figure 25

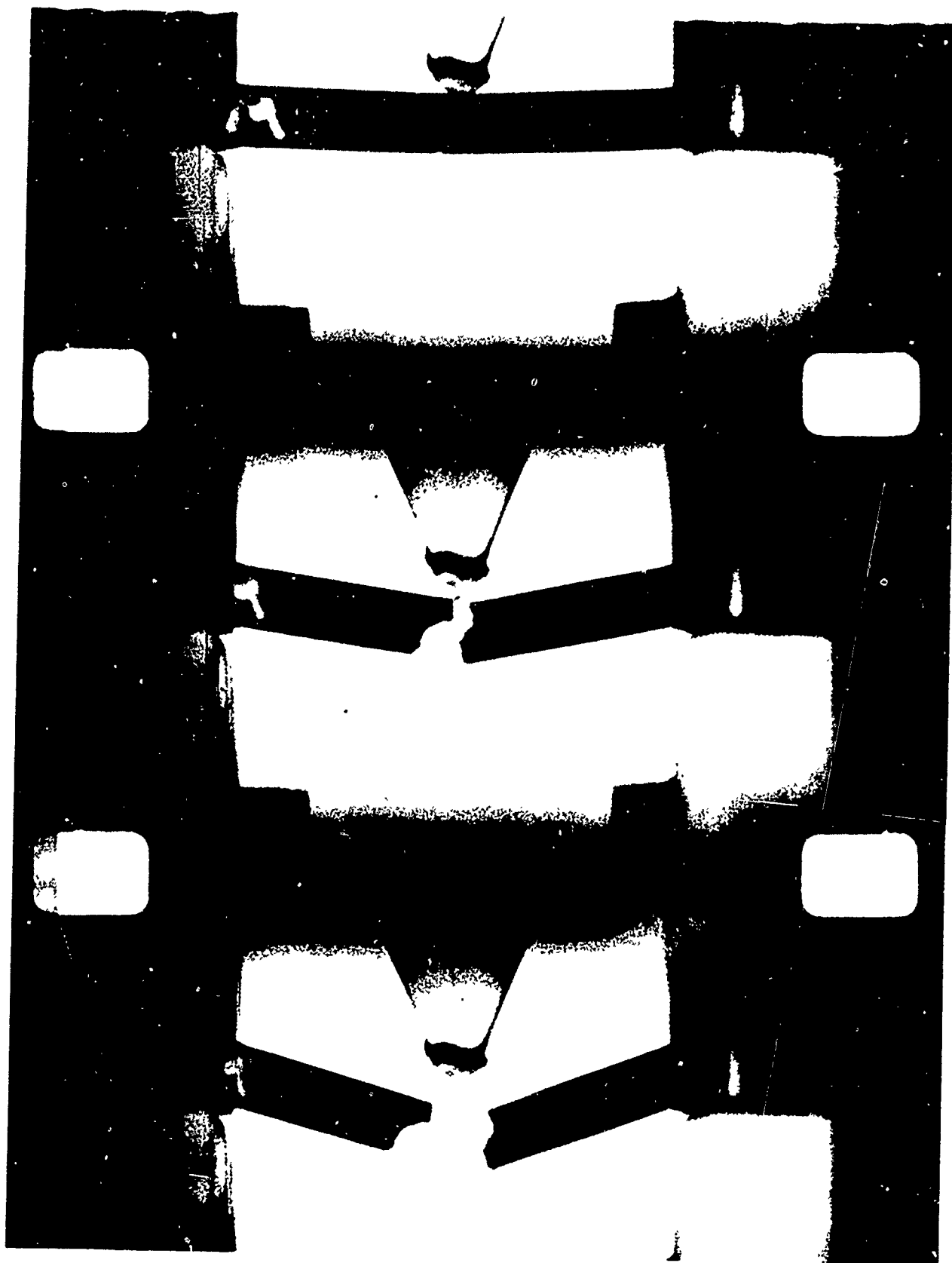


Figure 26

Frames from High Speed Movie Camera Showing Crack Propagation Through HMS Carbon Fiber Composite. Time interval between frames is 0.16 milliseconds.

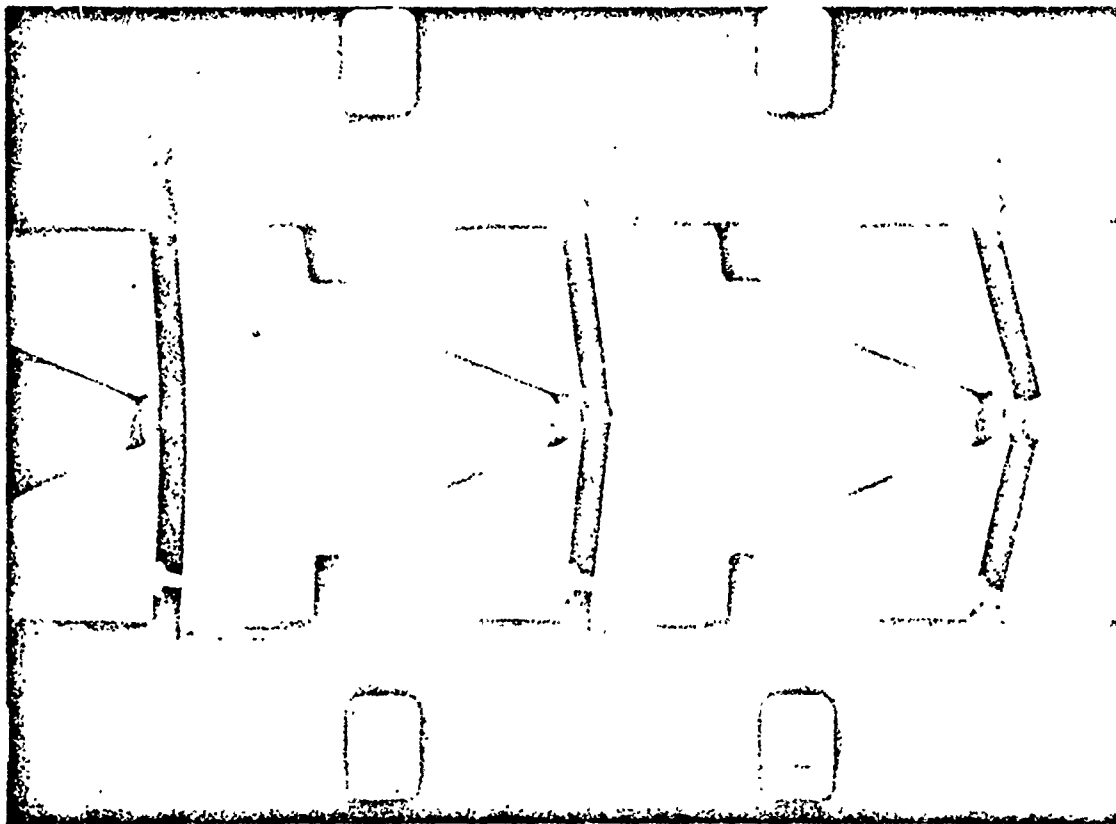
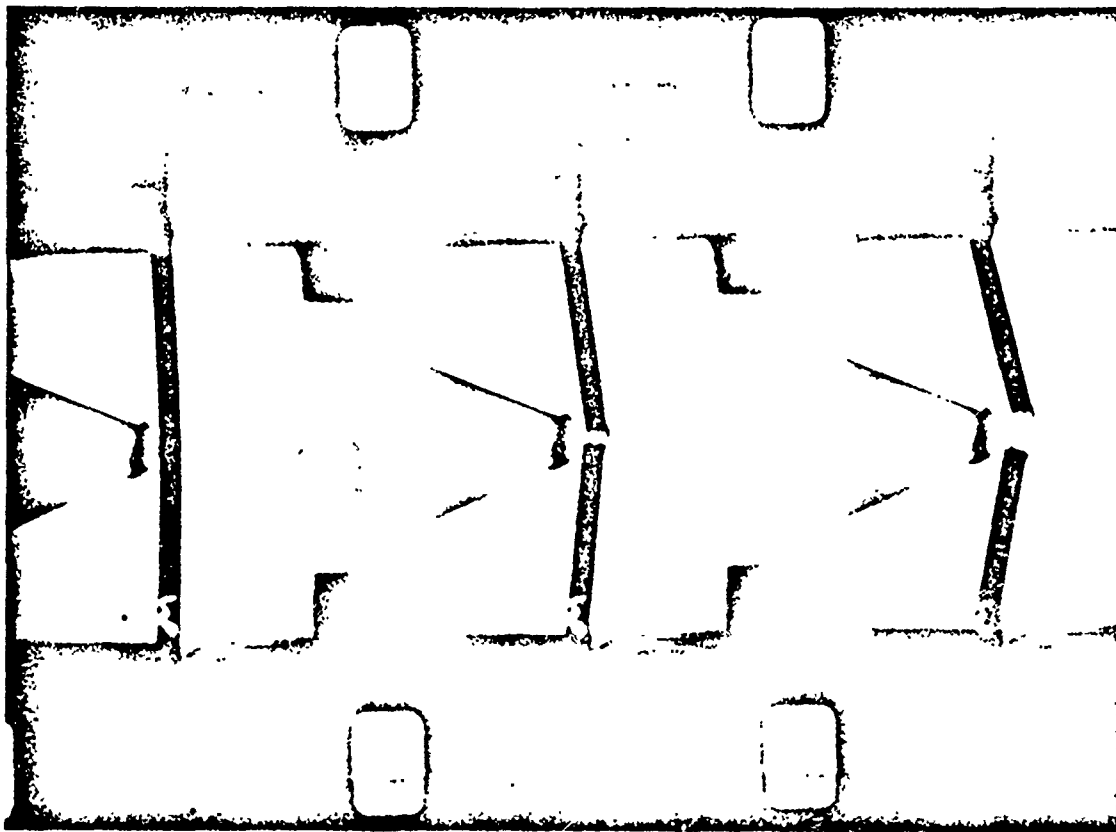


Figure 27 Frames from High Speed Movie Camera Showing Fracture of HMS Carbon Fiber Composite (left) and HTS Carbon Fiber Composite (right)

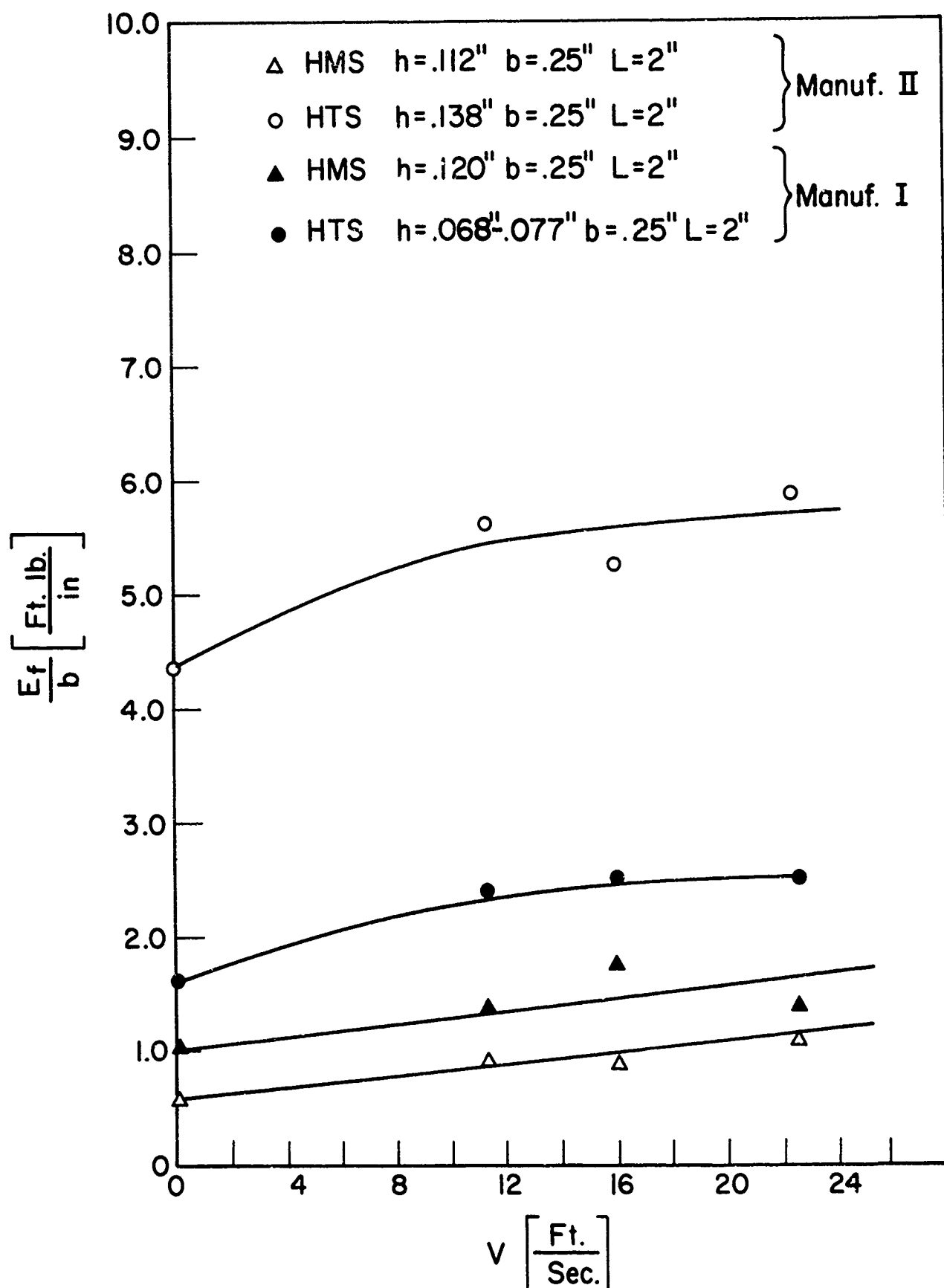


Figure 28

Energy Absorption of Carbon Fiber Composites as a Function of Loading Rate

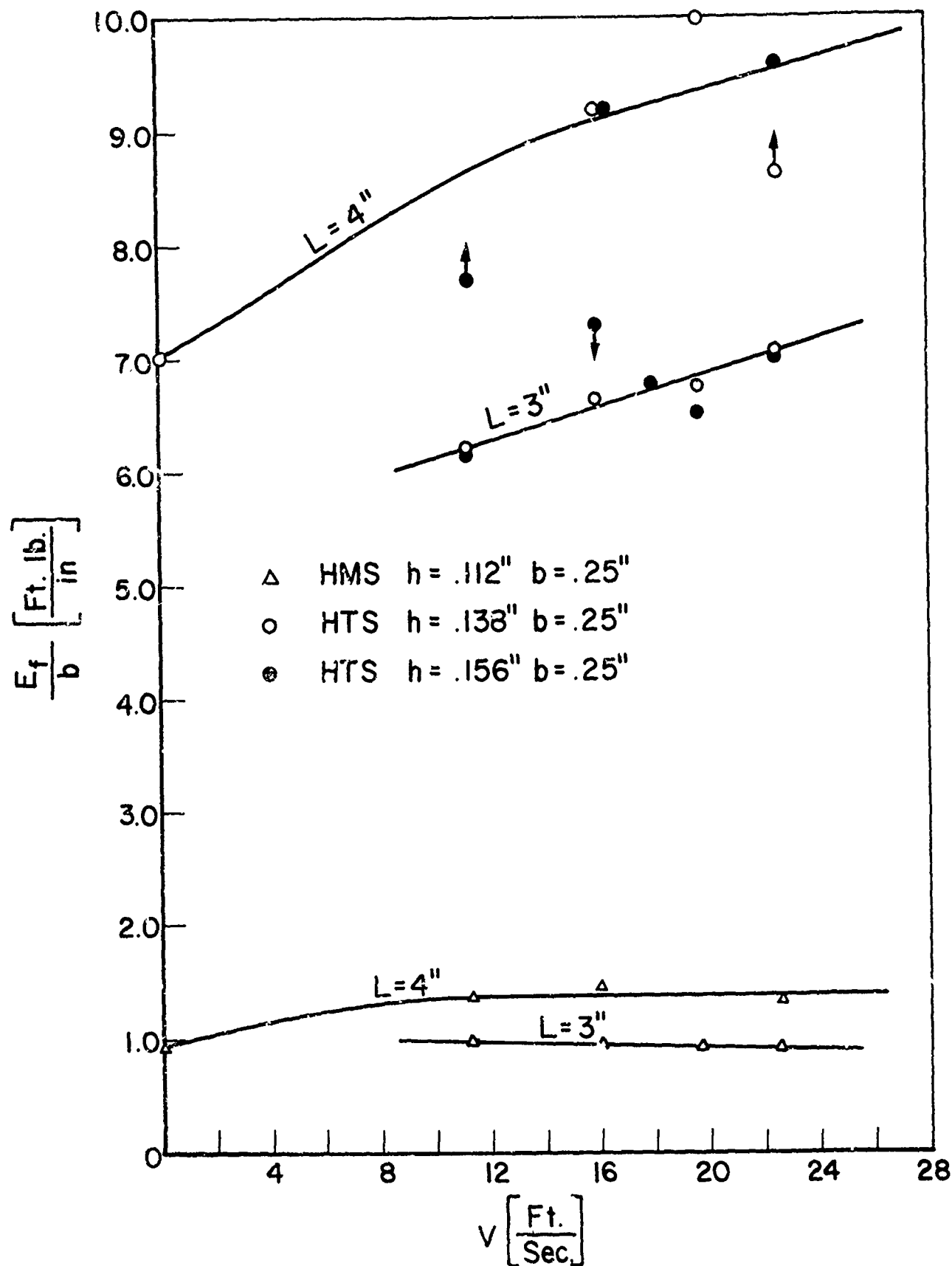
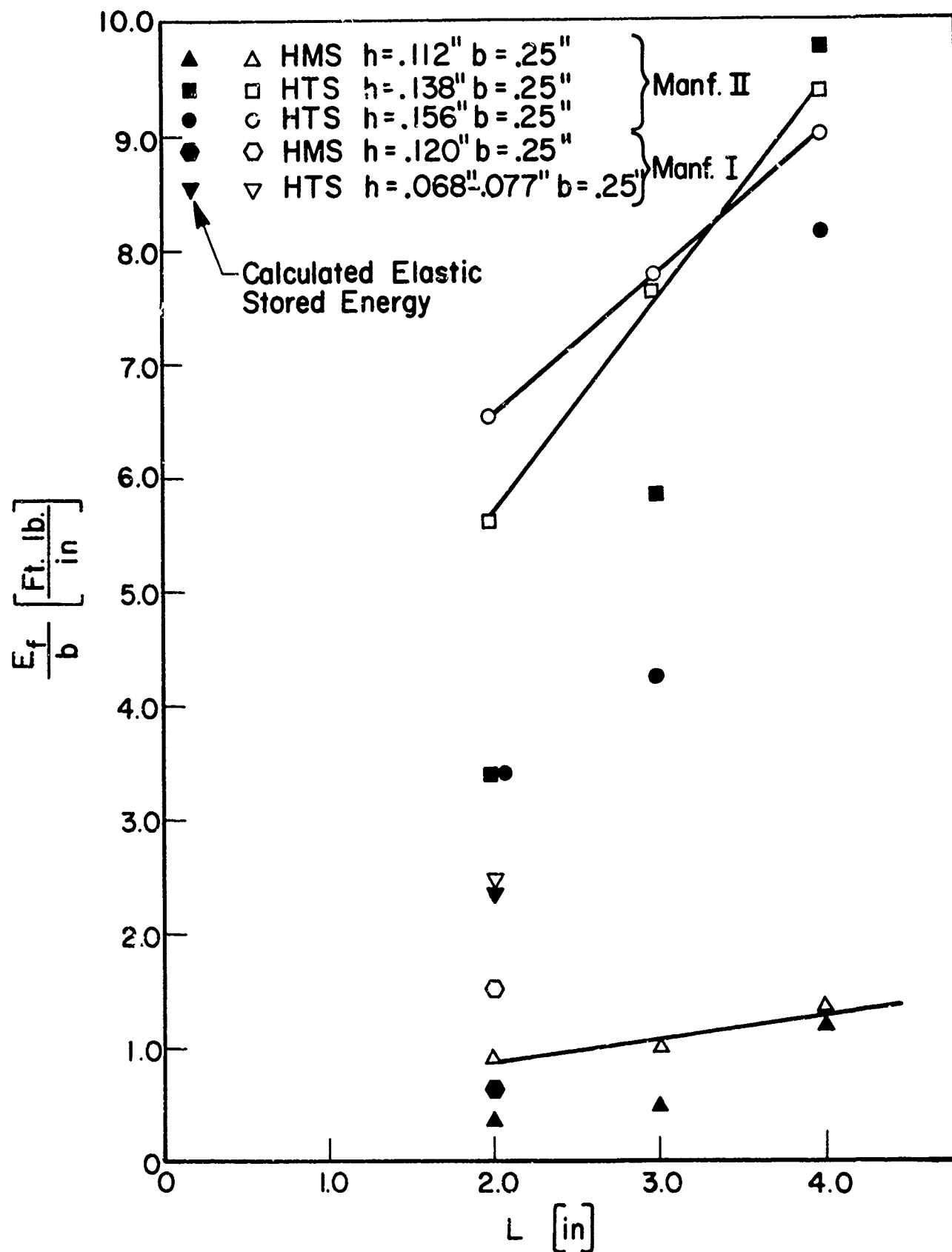


Figure 29

Energy Absorption of Carbon Fiber Composites as a Function of Beam Span and Loading Rate



48

Figure 30

Energy Absorption of Carbon Fiber Composites as a Function of Beam Span